Hydrological Processes

WILEY

RESEARCH ARTICLE OPEN ACCESS

Modelling the Effects of Wetland Restoration on Coastal Hydrology: A Case Study of Elkhorn Slough Watershed, California

Yi Xu[1,2] | Yu Zhang[2] | J. David Moulton[3] | Ashley Brereton[1,4] | Zelalem A. Mekonnen[4] | Bhavna Arora[5] | Charlie Endris[6,7] | John Haskins[7] | Adina Paytan[1]

[1]Earth and Planetary Sciences Department, University of California Santa Cruz, Santa Cruz, California, USA | [2]Earth and Environmental Science Division, Los Alamos National Laboratory, Los Alamos, New Mexico, USA | [3]Theoretical Division, Los Alamos National Laboratory, Los Alamos, New Mexico, USA | [4]Climate and Ecosystem Sciences Division, Lawrence Berkeley National Laboratory, Berkeley, California, USA | [5]Energy Geosciences Division, Lawrence Berkeley National Laboratory, Berkeley, California, USA | [6]Moss Landing Marine Laboratories, San Jose State University, Moss Landing, California, USA | [7]Elkhorn Slough National Estuarine Research Reserve, Moss Landing, California, USA

Correspondence: Yi Xu (yxu294@ucsc.edu) | Yu Zhang (zysight@gmail.com)

Received: 20 May 2025 | **Revised:** 22 October 2025 | **Accepted:** 24 October 2025

Keywords: advanced terrestrial simulator | coastal hydrologic modelling | coastal wetland restoration | hydrological processes | sea level rise

ABSTRACT

Coastal wetlands, some of the most productive ecosystems on Earth, provide critical ecosystem services, including support of biodiversity, carbon sequestration and flood protection. In recent decades, these ecosystems have experienced extensive coastal wetland loss. Coastal wetland restoration provides a beacon of hope, offering a chance to reclaim these important habitats. However, even with billions of dollars invested worldwide in restoring coastal wetlands, we still lack comprehensive knowledge about the effectiveness of these restoration efforts in recovering wetland ecosystem functions and how future climate change may affect these efforts. The ability to evaluate how these ecosystems will function in the future is vital for examining current investments and developing future protection and management plans. We selected Elkhorn Slough, a tidal estuary, in California, to investigate the impact of wetland restoration and sea level rise (SLR) on coastal hydrology using the process-based coastal hydrologic model, Advanced Terrestrial Simulator (ATS), informed by site-specific data. We designed a novel modelling workflow for incorporating wetland restoration features into land cover and soil properties for the model parameterization. The validation results demonstrate a strong agreement between modelled and observed data. We studied the characteristics of coastal watershed hydrology, then focused on the surface water dynamics at two wetland sites within Elkhorn Slough, a reference site and a restored site. Our simulation results indicate that the restored site successfully maintains surface elevation, resulting in reduced surface inundation. We also examined the impact of wetland restoration under expected SLR over the next few decades. The low-lying Yampah Marsh, the reference site, is likely to be inundated due to future SLR when highest tides arrive, while a higher percentage of Hester Marsh, the restored site, would retain marsh vegetation in coming decades, regardless of tidal conditions. Our study provides important information for examining the outcome of restoration practices that include surface elevation in tidal wetlands under climate changes.

1 | Introduction

Coastal wetlands are ecosystems situated at the interface between land and ocean. The hydrology of most coastal wetlands is impacted by tidal fluctuations in addition to precipitation, surface runoff and subsurface flow. Their proximity to the ocean subjects them to unique environmental conditions. Coastal wetlands also tend to be receptors and sinks of various

chemicals, including nutrients, trace metals, organic carbon, and anthropogenic pollutants. These dynamics are governed by hydrologic connectivity and upstream–coastal–ocean interactions (Cavalcante et al. 2020; Grande et al. 2022; Niu et al. 2021; Zhang et al. 2023, 2018). However, these same hydrologic and biogeochemical linkages also make coastal wetlands highly sensitive to human disturbances and climate-driven changes. During the 20th century, coastal wetlands lost more than half of their area worldwide due to human activities, including urban development, harbour construction, land reclamation for agriculture, saltwater intrusion and global sea level rise (SLR) (Kennish 2002; Li et al. 2018; Nicholls et al. 1999; Wasson et al. 2015; Yu et al. 2019). The loss of coastal wetlands reduces their ecosystem services including protection from storms and hurricanes, biodiversity, maintaining water quality, erosion control and carbon sequestration (Barbier 2013; Costanza et al. 2008; Li et al. 2018; Newton et al. 2012; Turner and Lewis 1996).

Coastal wetland restoration plays an important role in reclaiming these important habitats and restoring the ecosystem services they provide. With large investments in wetland restoration worldwide (Cadier et al. 2020), it is vital to understand the effectiveness of these restoration efforts in recovering wetland ecosystem functions and how these wetland systems will perform under future climate change. Understanding the restoration impact on coastal hydrology is an important first step because hydrologic processes are among the primary drivers of wetland biogeochemistry, affecting geochemical, ecological, and geomorphological processes (Ardón et al. 2013; Grande et al. 2023; Guimond et al. 2025; Zhang et al. 2019). However, there remains a significant knowledge gap in understanding how wetland restoration influences coastal hydrology, primarily due to the lack of long-term observation and predictive tools capable of capturing system changes before and after wetland restoration. Without this knowledge, uncertainties remain high when making appropriate restoration plans, optimizing investments, and minimizing irreversible coastal damage.

Numerical models offer an effective approach to address this knowledge gap as they can simulate complex hydrologic responses over varying spatial and temporal scales, which are not accessible through observation alone; a few studies have investigated the impacts of restoration on different wetlands using models.

Many numerical models have been developed and used to understand coastal hydrology at different scales. For example, a two-dimensional (2D) model was used to simulate the tidal fluctuations of a coastal groundwater table, incorporating the surface recharge driven by tides as well as the freely fluctuating water table within a coastal aquifer (Li et al. 1997). At the watershed scale, the FLATWOODS (Sun et al. 1998) and MIKE SHE (Dhi 2005) models have been used to investigate the variability in groundwater table dynamics and evapotranspiration of coastal forested watersheds under different climatic conditions (Dai et al. 2010; Sun et al. 1998). At the regional scale, PIHM-Wetland, a physically based model that integrates upland surface and subsurface hydrology, coastal hydrology, and near-coast ocean processes, is able to examine how upland-coast hydrologic connectivity affects coastal surface and subsurface water discharge and saltwater intrusion (Zhang et al. 2018). Such improved representation of coastal hydrological connectivity also enhanced the quantification of coastal hydrological resilience to identify thresholds at which droughts and storms trigger groundwater decline and widespread flooding (Zhang et al. 2019).

Only a few studies have employed models to evaluate hydrological changes in wetlands following restoration. An example is the study of the impact of coastal wetland restoration on hydrological components (rainfall, evapotranspiration, runoff, streamflow, etc.) in the Heeia watershed, Hawaii (Ghazal et al. 2020), using the Soil and Water Assessment Tool (SWAT) (Arnold et al. 1998). Results indicated that land cover conversion (e.g., from grassland to taro fields) may lead to reductions in baseflow and streamflow within the watershed. Another example is the development of the Coastal Wetland Equilibrium Model (CWEM) to assess future marsh function (Morris et al. 2002, 2021). For instance, CWEM has been integrated with organic matter content and peat age to examine tidal wetland evolution and resilience under varying SLR scenarios in the Sacramento–San Joaquin Delta, California (Morris et al. 2022). While CWEM has also been used to evaluate the effects of enhanced surface elevation in tidal wetlands after restoration, it did not incorporate detailed hydrodynamic processes, such as evapotranspiration, infiltration, surface runoff, or tidal flow (Harris et al. 2025). Some other studies focused specifically on coastal wetland restoration impacts on carbon dynamics (Eagle et al. 2022) and the relationship among carbon sequestration, methane emissions and soil accretion (Arias-Ortiz et al. 2021), but not on climate change impacts or related hydrological changes on these ecosystem functions. Some studies also investigated the impact of restoration on hydrology in non-tidal wetlands. For example, Groundwater Vistas (GWV) v3 derived from the MODFLOW code (McDonald and Harbaugh 1988) was applied at Tadham Moor, UK and it used a 2D transect to model the effectiveness of ditch water levels in influencing wetland water table levels at this non-tidal wetland (Acreman et al. 2007).

To our knowledge, there is still a lack of investigation into the impact of surface elevation changes related to wetland restoration on coastal wetland hydrology, which introduces a considerable challenge to understanding the hydrologic dynamics and the fate of coastal wetlands under future climate change, like SLR. In this study, we selected Elkhorn Slough, a tidal estuary in California, as our study site to investigate the impacts of wetland restoration on coastal hydrology. We used the coastal hydrology configuration from the Advanced Terrestrial Simulator (ATS), a multi-physics model, to simulate coupled surface and subsurface hydrologic processes in a coastal setting with tidal variations (Coon et al. 2016, 2019; Zhang et al. 2022). In particular, we incorporated wetland restoration features into land cover and soil properties of the modeled sites within the Elkhorn Slough watershed to examine the impact of wetland restoration on coastal wetland hydrology under current climate and future SLR scenarios. We specifically explored the following scientific questions: (1) How does wetland restoration impact the hydrological processes of the coastal wetlands under the current climate regime? and (2) How resilient are restored wetlands to future SLR?

2 | Model Description and Study Site

2.1 | Numerical Model

The ATS model is a spatially distributed, process-based model. For this model Coon et al. (2016) formalised the Arcos multi-physics framework—organising process equations into a hierarchical process tree with automated weak and strong coupling strategies. Subsequently, a major upgrade by Coon et al. (2020) introduced a face-based mimetic finite difference approach for tightly coupling surface flow and subsurface flow on unstructured meshes. The ATS model tracks the time rate of change of water storage on the land surface and subsurface as a function of evapotranspiration, infiltration, recharge, surface flow and subsurface flow. Potential evaporation and transpiration are calculated using a modified form of the Priestley–Taylor equation (Priestley and Taylor 1972). Specifically, the surface flow is simulated using a two-dimensional (2-D) diffusive-wave approximation (Lal 1998; Vreugdenhil 1994), while the subsurface water change is represented using a variably saturated three-dimensional (3-D) Richards equation (Richards 1931), which also accounts for the infiltration process. More model details can be found in Equations (1–3). Specifically, coastal processes, such as coastal tidal variation, saltwater intrusion, and storm surge have been incorporated into ATS (Zhang et al. 2022). These coastal processes can be represented by combining boundary conditions, surface-subsurface coupling and process modules. We note that tidal variation is one of the most important processes in coastal watershed hydrology. To capture tidal forcing, the tidal variations can be applied at the land-ocean interface, which influences both surface and subsurface flow. Equations describing these relevant hydrological processes have been presented in prior research (Zhang et al. 2022) and are therefore not reiterated in this work. Details of the model setup for this study are provided in Section 2.3.1.

2.1.1 | Surface Flow

Surface water was estimated using a diffusion wave scheme for water balance on the surface (Lal 1998; Vreugdenhil 1994):

$$\frac{\partial h}{\partial t} + \nabla_s \cdot h\overrightarrow{q_s} = q_{ss} + q_e \tag{1}$$

where h represents the surface water depth (m), t is the time (s), ∇_s is the 2-D surface gradient (m^{-1}), $\overrightarrow{q_s}$ is the 2-D flux field ($m\,s^{-1}$), q_{ss} is the flux between subsurface and surface systems such as exfiltration or infiltration ($m\,s^{-1}$) and q_e is external source term (e.g., rainfall) ($m\,s^{-1}$).

2.1.2 | Subsurface Flow

In ATS, subsurface flow was represented by the Richards equation for variably saturated flow (Coon et al. 2020):

$$\frac{\partial}{\partial t}(\phi S) + \nabla \cdot \vec{q} = 0 \tag{2}$$

with

$$\vec{q} = -\frac{1}{\mu} k_r \kappa \left(\nabla p + \rho \vec{g} \right) \tag{3}$$

where S is the saturation of water (–), ϕ represents the effective soil matrix porosity (–), $\vec{q}$ is the Darcy flux ($m\,s^{-1}$), k_r is the relative permeability (–), κ is the absolute permeability (m^2), μ is the dynamic viscosity (Pa s), p is the water pressure (Pa), $\vec{g}$ is the vector of gravity ($m\,s^{-2}$) and ρ is the mass density of water ($kg\,m^{-3}$).

2.2 | Study Site and Data

2.2.1 | Study Site

Elkhorn Slough watershed (ESW) (38.7 km^2), lies within a low-relief coastal terrain, extending from upland terraces and the foothills of the Gabilan Range down to the tidal estuary that terminates in Monterey Bay, California (Figure 1a). This site has an average annual rainfall of around 55.2 cm, and most of the precipitation concentrates between October and May (Caffrey et al. 2002; Montalvo et al. 2024). Over the past several centuries, tidal marsh loss has been driven by anthropogenic activities, including diking, marsh drainage for agricultural purposes and the construction of the Moss Landing harbour at the wetland mouth. Sediment supply has declined due to the damming of the Pajaro River, the diversion of the Salinas River and the construction of the Moss Landing harbour (Wasson et al. 2015; Watson et al. 2011). These anthropogenic modifications have contributed to a long-term historical reduction in the surface elevation of the natural marsh. Due to these changes and the resulting sediment supply reduction, some areas of the slough have subsided and become inundated mudflats (Fountain et al. 2022). However, in recent decades (2006 to present), Elkhorn Slough, except for the restored site, has not seen many additional changes. The measurement from Surface Elevation Tables (SETs) indicates a slight surface elevation gain occurs in Elkhorn Slough, resulting from the combined effects of natural subsurface processes, surface accretion and subsidence (more detailed information is provided in Section 2.3.3). But this slight surface elevation increase cannot keep pace with expected SLR.

Wetland restoration projects were implemented at Elkhorn Slough to restore the natural condition of some of the degraded wetlands (converting from mudflats to vegetated wetlands) and sustain the marsh for decades to come. At Hester Marsh, a formerly diked and drained marsh, the elevation prior to restoration was slightly above mean sea level (Figure 1b) and too low to support wetland vegetation. The entire Hester Marsh restoration area managed by the Elkhorn Slough National Estuarine Research Reserve (ESNERR), includes Hester Marsh, Minhoto Marsh and Seal Bend Marsh. Phase 1 of the restoration at Hester Marsh (the area defined by the pink-line polygon in Figure 1a, 0.30 km^2) took place between December 2017 and March 2019 and included diking, dredging, earth moving and planting. Phase 2 of the Hester Marsh restoration project at Minhoto Marsh (the area defined by the rose-line

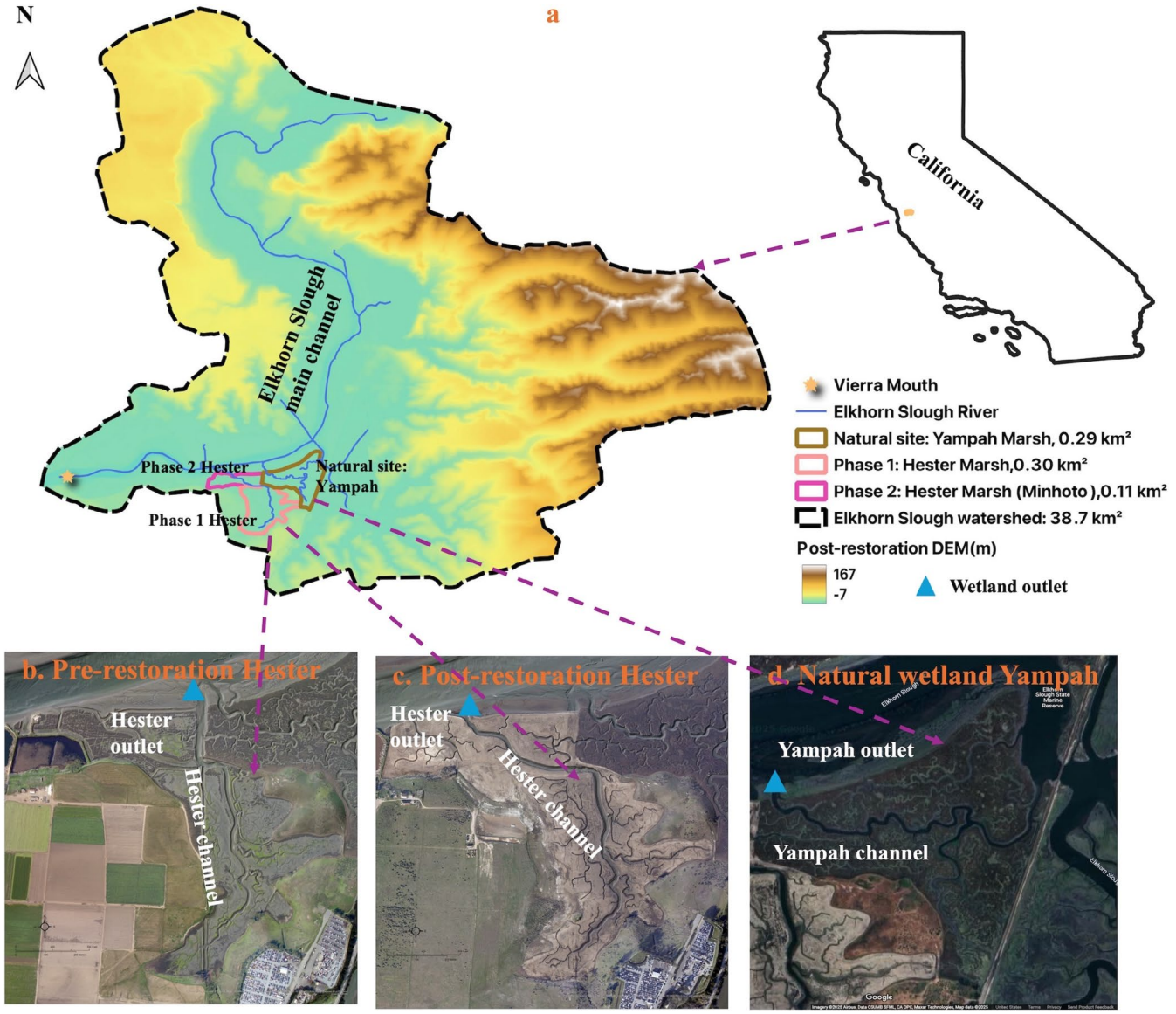

FIGURE 1 | Location of the study area: (a) Elkhorn Slough watershed with stream networks, Yampah Marsh and Hester Marsh (includes Phase 1 Hester and Phase 2 Hester) (basemap credit: 2010 Light Detection and Ranging data, 1 m resolution); (b) Hester Marsh pre-restoration status in 2012 (Fountain et al. 2022); (c) Hester Marsh post-restoration status in 2022 (Fountain et al. 2022); and (d) Yampah Marsh (natural wetland), map credit: Imagery ©2025 Airbus, Data CSUMB SFML, CA OPC, Maxar Technologies, Map data ©2025 Google. The watershed boundary is from the Elkhorn Slough Reserve website (https://elkhornslough.org/reserve/).

polygon in Figure 1a, 0.11 km^2) occurred between August 2020 and 2022 (Fountain et al. 2022). Phase 1 Hester Marsh and Phase 2 Hester Marsh (i.e., Minhoto Marsh) are hereinafter collectively referred to as Hester Marsh (Figure 1c, 0.41 km^2 in total). The marsh fill materials used in Phase 1 and Phase 2 were sourced from sediments extracted from the adjacent hillside to the west of Phase 1 area and from a nearby flood control project at Pajaro river (Fountain et al. 2022). One of the main targets for this restoration project was to raise Hester Marsh to an elevation well above Mean Higher High Water (MHHW, i.e., 1.76 m above the North American Vertical Datum of 1988 (i.e., NAVD88)) in order to reclaim tidal marsh habitats and protect the site from future SLR. Additionally, the previous channel section near the Hester outlet was cut off and filled with sediment, and a man-made channel section was constructed at Hester Marsh based on historical records, shifting the outlet location of the Hester channel (Figure 1b,c); while most of the inland channels within Hester Marsh remained unchanged before and after restoration. Details of the plan and technical approaches of the restoration can be found in Fountain et al. (2022). Yampah Marsh (the area defined by the brown-line polygon in Figure 1a, 0.29 km^2) has not been altered by the restoration project and still retains its natural conditions. Thus, Yampah Marsh, a nearby site which has never been diked or drained, was used as a reference natural wetland in this study. Since the vegetation in Hester Marsh is still in its early stages of establishment, the vegetation cover in the restored area has a relatively minor influence on the hydrological processes. Therefore, we focused more on examining the impact of the elevation change on the hydrology. We define the pre-restoration scenario as the conditions before Phase 1 of the Hester restoration (prior to 2018), while the

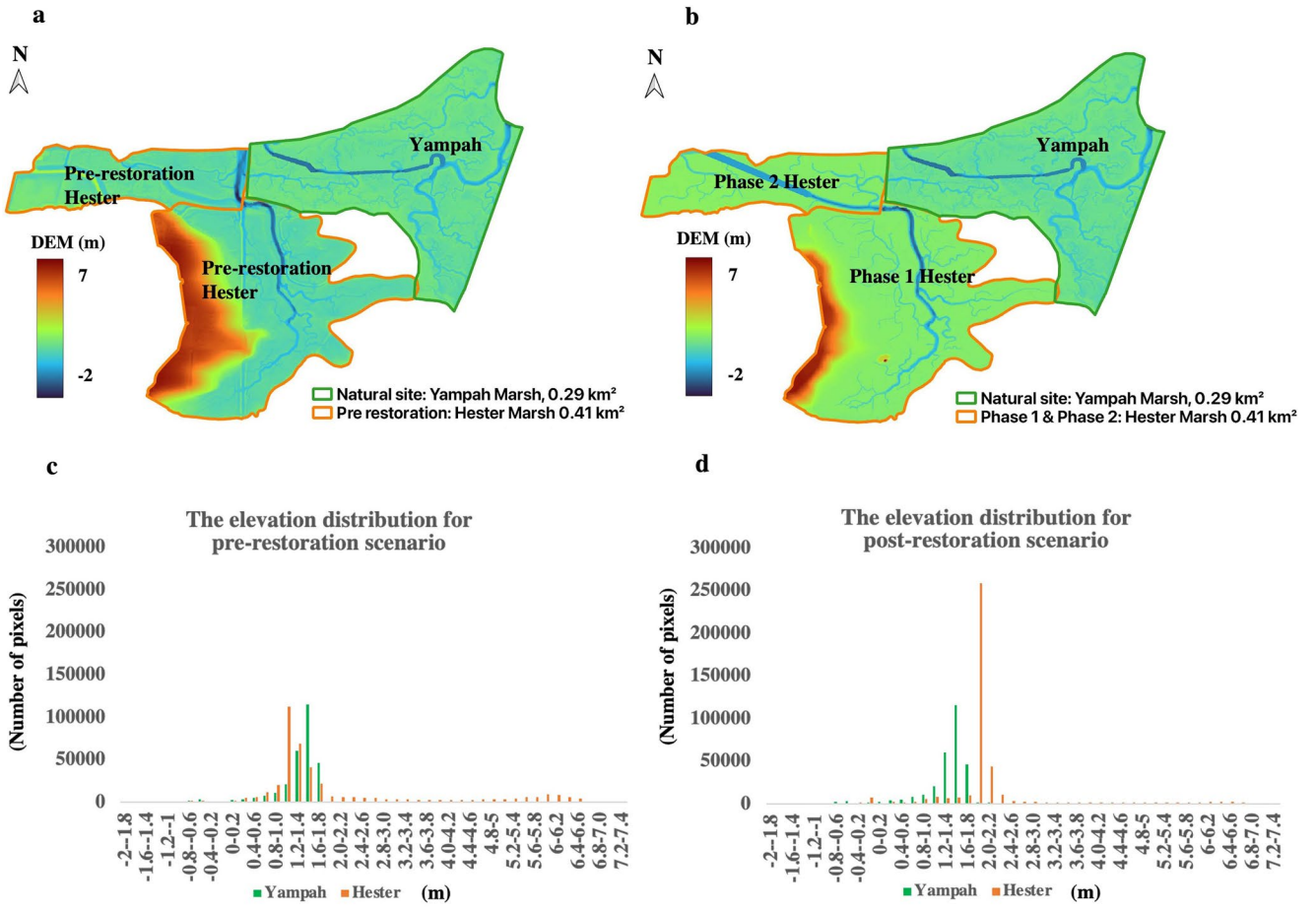

FIGURE 2 | (a) Pre-restoration DEM of Yampah Marsh and Hester Marsh; (b) post-restoration DEM of Yampah Marsh and Hester Marsh; (c) the elevation distributions for the pre-restoration scenario of Yampah Marsh and Hester Marsh; (d) the elevation distributions for the post-restoration scenario of Yampah Marsh and Hester Marsh. The high-elevation hill located along the western boundary of Phase 1 Hester Marsh served as a soil source for marsh fill during restoration. The datums of both pre- and post-restoration DEMs are referenced to NAVD88 (meters).

post-restoration scenario is a scenario after Phase 1 and Phase 2 of the Hester restoration (post 2022).

The surface elevation was derived from a bare-earth digital elevation model (DEM). The pre-restoration DEM of the watershed was derived from a mosaic of a 2011 multibeam bathymetry dataset (CSUMB Seafloor Mapping Lab) and the 2010 Light Detection and Ranging (LiDAR) dataset (1 m resolution), collected via an airborne collection platform during a survey of Coastal California (Office for Coastal Management 2025). Following the restoration project, a new DEM was generated by integrating a mosaic of unmanned aerial vehicle (UAV) structure from motion (SfM) elevation data of the restored Hester Marsh (Phase 1 and Phase 2) collected in 2018 and 2021 with the pre-restoration DEM of the watershed outside the restoration area. We defined this new DEM as the post-restoration DEM for Elkhorn Slough. Both pre-restoration and post-restoration DEMs are available at the California State University ScholarWorks website (http://hdl.handle.net/20.500.12680/41687t28s).

The comparison of surface elevations between Hester Marsh and Yampah Marsh reveals notable differences before and after the restoration for Hester Marsh, as expected (Figure 2a,b). The elevation of Yampah remained relatively stable between the two periods (the green bars in Figure 2c,d), with most of its elevation distribution concentrated between 1.2 and 1.8 m. For Hester Marsh, the elevation change is more significant (the orange bars in Figure 2c,d). Before restoration, the elevation distribution of Hester Marsh was primarily within the range of 0.8–1.6 m (Figure 2c), indicating that most of its surface elevations were lower than those of Yampah Marsh. In contrast, after the restoration project, the elevation at the western upland area of Phase 1 Hester Marsh became lower (where the soil for fill was excavated), while the elevation of Phase 1 eastern Hester Marsh and Phase 2 Hester Marsh increased due to sediment redistribution. Post-restoration elevation distributions (Figure 2d) indicate that most surface elevations at Hester Marsh now range between 1.8 and 2.2 m, which is higher than the majority of surface elevations observed at Yampah Marsh.

In this study, we account for both the influence of water inflows from the upland watershed hills (the brownish regions in Figure 1a) and the hydrological changes in the marsh lowlands driven by tidal fluctuations. We first simulated surface and subsurface hydrological processes to understand the hydrologic characteristics of the watershed. Subsequently, we focused on Yampah Marsh and Hester Marsh to assess the impact of restoration on coastal wetland hydrology by comparing hydrological changes between the two marshes.

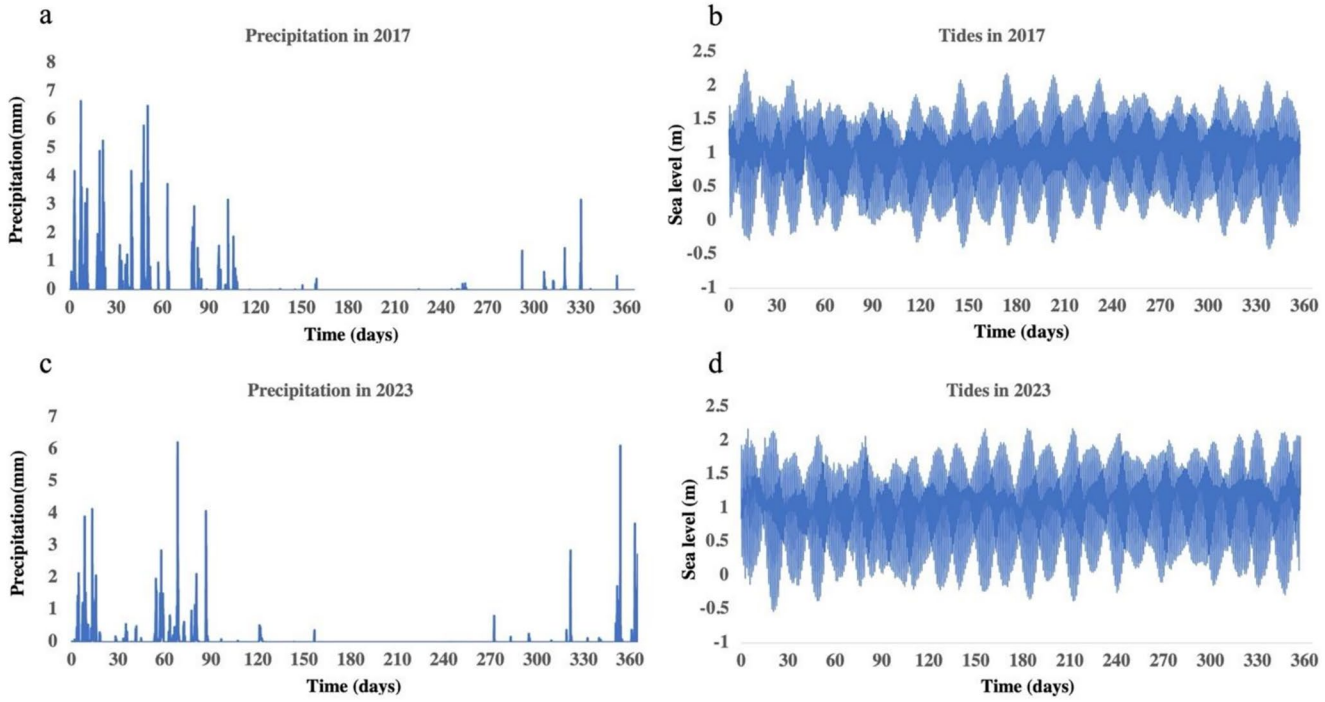

FIGURE 3 | (a) Precipitation (NLDAS-2 product) and (b) tides in 2017; (c) precipitation (NLDAS-2 product) and (d) tides in 2023.

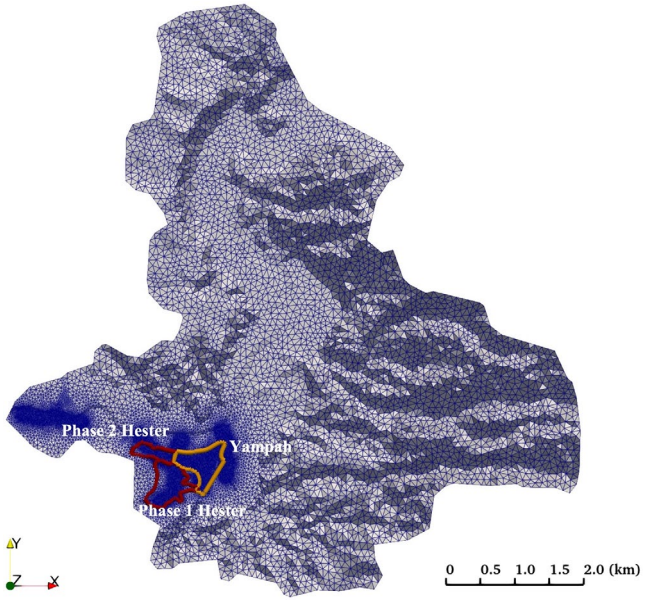

FIGURE 4 | ATS mesh for the Elkhorn Slough watershed. The horizontal scale bar represents planimetric distance. For visualisation purposes, the vertical dimension Z is exaggerated by a factor of 10 relative to the horizontal scale (i.e., a vertical-to-horizontal scale ratio of 10:1).

2.2.2 | Data

We used the meteorological forcing data from the North American Land Data Assimilation System Phase 2 (NLDAS-2) (Xia et al. 2012) and tidal water level data (referenced to NAVD88) from the NOAA Tides and Currents website at the Monterey Station (https://tidesandcurrents.noaa.gov/map/index.shtml) to drive the model simulations. The meteorological forcing includes precipitation, air temperature, shortwave radiation and vapour pressure. Our numerical experiments include the hydrology simulations for the pre-restoration conditions in 2017 and the post-restoration conditions in 2023. The reason for selecting 2017 as the pre-restoration case is that the winter of 2017 delivered very heavy precipitation to most of Monterey County resulting in severe floods (County of Monterey 2024). This facilitates the evaluation of the model response to wet seasons. Year 2017 served as the baseline, preceding the initiation of Phase 1 restoration on December 11, 2017. We confirmed that there was no earth-moving from December 11 to 31, 2017. To assess the post-restoration effects, 2023 was selected, as it represents the conditions 1 year after Phase 2 restoration ended. The hourly precipitation and tidal dataset for 2017 are presented in Figure 3a,b, while those for 2023 are depicted in Figure 3c,d, respectively.

To generate the mesh and incorporate the landscape information, we used the ATS model mesh generation tool, Watershed Workflow (Coon and Shuai 2022). The watershed domain was decomposed into a 3-D unstructured triangular mesh with a surface resolution (defined as the average triangle edge length) ranging from 5 m to over 100 m (e.g., the post-restoration mesh is shown in Figure 4) including around 390 000 cells to capture the variations in surface elevation and land cover features, together with 8 subsurface layers. The shape of the pre-restoration mesh is similar to the post-restoration mesh. The mesh size near the watershed outlet and the wetland areas was finer than the other areas in the watershed to capture fine landscape details within the channels. Watershed Workflow also incorporates soil type, soil thickness and geology information from the national datasets into the ATS mesh. Specifically, Watershed Workflow uses the DEM dataset from NOAA (Office for Coastal Management 2025), the river network data from National Hydrography Dataset Plus (NHDPlus) (Simley and Carswell Jr 2009), the land cover data from National Land Cover Database (NLCD) (Homer et al. 2012), the soil data

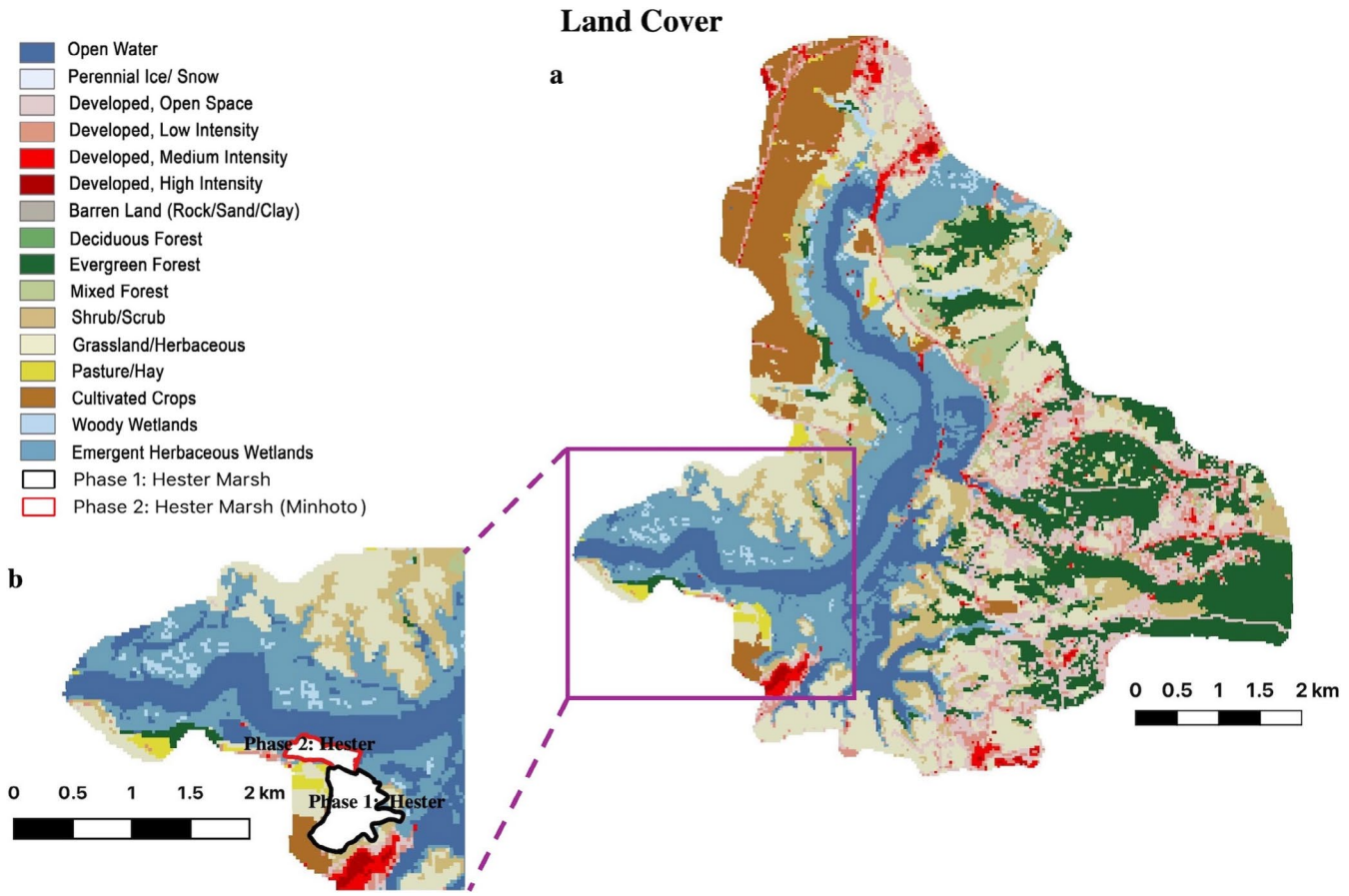

FIGURE 5 | (a) Land cover index for the pre-restoration scenario; (b) modified land cover for the post-restoration scenario, designating the restored Hester area for Phase 1 and Phase 2 as a restoration land cover type.

from Soil Survey Geographic Database (SSURGO) (Soil Survey Staff 2021), the soil depth data from the SoilGrids 2017 depth-to-bedrock field (Shangguan et al. 2017) and the geology data from GLobal Hydrogeology MaPS version 2.0 (GLHYMPS) (Huscroft et al. 2018a, 2018b).

To better represent the wetland restoration area, we modified the existing land cover data and soil data to better reflect both the pre- and post-restoration conditions. We used the NLCD data from 2016 as the land cover data for the pre-restoration case (Figure 5a) and the NLCD 2021 as the land cover for the post-restoration case. However, the NLCD 2021 is similar to NLCD 2016 throughout the watershed, which is not accurate enough to represent the post-restoration land cover, because the restored area at Hester Marsh site is different from well-established natural herbaceous wetlands. Therefore, we manually added a new restored wetland category in NLCD 2021 to accurately represent the actual land cover conditions at the restored Hester Marsh (Figure 5b).

For the soil data, with the restoration practice, the soil properties have significantly changed compared to the soil properties in SSURGO because the dredged soil was added at the surface, and the soil was compressed by heavy machinery during the marsh fill. Specifically, the surface layer of added fill at the restored wetland is organic matter poor, sandy and silty soil, while the bottom layer is less disturbed retaining the soil typical of natural wetlands (Fountain et al. 2022). In the natural wetland, Yampah, the surface layer (i.e., slurry layer) has high water content, while the bottom layer is incompressible clay, and the soil has high organic matter content. Therefore, we utilised the vector-based SSURGO data for the pre- and post-restoration periods for Yampah Marsh and only for the pre-restoration period for Hester Marsh. We modified SSURGO data for the post-restoration case to provide more accurate soil texture information for the restored wetland site at Hester Marsh, based on the available field measurements (Table 1).

2.3 | Numerical Experimental Design

2.3.1 | Model Setup

The model setup for both pre- and post-restoration scenarios consists of several key steps:

2.3.1.1 | Mesh Generation. Constructing computational meshes (similar to Figure 4) is a critical step, incorporating the modelling domain, stream networks, DEM, land cover, and soil information. The primary differences between the pre- and post-restoration meshes arise from the changes in DEM, stream networks, land cover, and soil characteristics around Hester Marsh following the restoration project, as described in Section 2.2.

TABLE 1 | Soil properties for the natural and restored wetland soils.

Soil properties	Sand (%)	Clay (%)	Silt (%)
Natural soil: Yampah Marsh and pre-restoration Hester Marsh	37.6	26.6	35.8
Restored soil: post-restoration Hester Marsh	69.4	6.2	24.4

2.3.1.2 | **Model Configuration.** The ATS configuration is defined within an XML file, specifying key parameters and settings: initial time step was set to 1 s (with time step adaptation enabled in ATS); output time step was set to hourly intervals; subsurface initial conditions were assumed to be fully saturated; the initial surface ponded water depth was set to 0 m; open boundary conditions were applied at the land–ocean interface, where tidal water levels (referenced to NAVD88) were prescribed as Dirichlet boundary conditions for both surface and subsurface flow. This setup allows the model to simulate hydrologic interactions across the land–ocean interface, driven by tidal fluctuations. This open boundary at the watershed outlet serves as the sole land–ocean connection in the study domain. For the remaining inland boundaries of the Elkhorn Slough watershed, we implemented closed boundary conditions for both surface and subsurface water. We note that in this specific watershed the inland groundwater level is several meters deep, and therefore the closed boundary condition for the inland boundary should have limited influence on the overall hydrologic change, especially the surface and groundwater flow near the land–ocean interface.

2.3.1.3 | **Model Spin-Up.** Meteorological forcing data for 2017 and 2023 were obtained from the NLDAS-2 products for the pre- and post-restoration scenarios, respectively, while tidal data for the same periods were sourced from NOAA observations at the Monterey Station. We firstly conducted a 1.5-year spin-up for both scenarios by using a constant tide to allow the model to reach equilibrium, after which the model was further spun up for 60 days with the corresponding real tidal dataset for both pre- and post-restoration scenarios. The spin-up results were subsequently employed as the restarting conditions of the transient model runs to efficiently minimize the impact of initial conditions.

2.3.2 | Analyses of the Hydrology Features at the Watershed and Wetland Sites Before and After Wetland Restoration

For the watershed scale analysis, we focused on the overall distributions of surface flood extent and groundwater table depth (GWT) under different conditions, reflecting the distinctions of the combined impact of precipitation and coastal tidal inundation conditions in the periods before and after wetland restoration. For the hydrologic analysis at the wetland sites, we focused on understanding the wetland restoration impact on wetland hydrology by comparing the differences in inundation extent and surface water depth between Hester Marsh and Yampah Marsh during the pre- and post-restoration periods. We did not examine the restoration impact on the hydrologic processes at the watershed scale because the restoration project concentrated on a relatively small area (only 1% of the watershed), making it unlikely to induce significant hydrological changes at the watershed scale, but posing noticeable local impact.

2.3.3 | Future Scenario With Sea Level Rise

After understanding the impact of wetland restoration on coastal hydrology under the current climate condition, we further investigated whether the restoration practice is sufficient in protecting coastal wetlands in the next several decades with the influence of accelerated SLR. We assessed the impact of SLR on the coastal wetland restoration by considering several future SLR scenarios. We therefore used the ATS model to evaluate the impact of SLR on Hester and Yampah marshes by comparing water inundation areas at the middle and the end of the 21st century (i.e., 2050 and 2100). For both years, two SLR scenarios were considered: an intermediate SLR scenario and a high SLR scenario, which were adopted from the work of Sweet et al. (2022). In the work of Sweet et al. (2022), every scenario has three sub-scenarios: low, medium and high value, corresponding to the 17th, 50th, and 83rd percentiles. We chose the 50th percentiles sub-scenarios for both intermediate and high SLR scenarios. In Table 2, the relative sea levels (RSL) referenced to year 2005 (columns 2 to 6) were obtained from the work of Sweet et al. (2022). The derived tidal level ranges of four future scenarios (i.e., 2050 intermediate SLR scenario, 2050 high SLR scenario, 2100 intermediate SLR scenario and 2100 high SLR scenario) are shown in columns 7 to 8 in Table 2. For all simulations tides were referenced for those at Monterey Station (ID: 9413450), CA.

We used the 2050 intermediate SRL scenario as an example to explain how we obtained the tidal level ranges in Table 2. First, we used 2023 (post-restoration scenario) as a baseline to calculate the projected SLR under the 2050 intermediate SLR scenario: $(20-5)-(9-5)/10\times(2023-2020)=14$ cm (we kept the consistent decimal accuracy with the numbers provided by Sweet et al. (2022)). Then we added the projected SLR to the 2023 tidal level range (i.e., −0.53 to 2.18 m) to derive projected tidal level range under the 2050 intermediate SLR scenario. The resulting tidal range under the 2050 intermediate SLR scenario was estimated to be between −0.39 and 2.32 m. The future tidal level ranges under all other scenarios were generated similarly and listed in Table 2. Most model parameters and configurations remain the same as those used in the model validation, with all the future scenarios driven only by the projected tidal conditions under future SLR. For all the future scenarios, we assumed no changes in land cover, soil properties and meteorological forcing variables (i.e., temperature, shortwave radiation and precipitation) and these datasets were obtained based on the post-restoration scenario (i.e., 2023), except for surface elevation.

Surface elevation at Elkhorn Slough is known to change over time due to subsurface processes, surface accretion and

TABLE 2 | The sea level and tidal range in 2050 and 2100 under the intermediate and high SLR scenarios from Sweet et al. 2022. Relative sea levels in columns 2 to 6 are referenced to year 2005 (Sweet et al. 2022), and tidal level ranges are provided in columns 7 to 8 for four future scenarios: (1) 2050 with an intermediate SLR scenario; (2) 2050 with a high SLR scenario; (3) 2100 with an intermediate SLR scenario; and (4) 2100 with a high SLR scenario.

Study site	RSL 2005 (cm)	RSL 2020 (cm)	RSL 2030 (cm)	RSL 2050 (cm)	RSL 2100 (cm)	2050 tidal ranges (m)	2100 tidal ranges (m)
Intermediate SLR scenario	0	5	9	20	88	(−0.39, 2.32)	(0.29, 3.00)
High SLR scenario	0	6	11	35	194	(−0.25, 2.46)	(1.34, 4.05)

Note: 2023 is a benchmark for future scenarios and the relevant tidal range is −0.53 to 2.18 m. Tidal level datum is NAVD88.

subsidence. SETs, installed at various locations in the watershed, provide precise measurements of these changes. SETs show four average surface elevation increasing rates at four sub-watersheds (1.48, 1.80, 1.57 and 2.25 mm/yr on Sub-watershed 1, Sub-watershed 2, Sub-watershed 3 and Sub-watershed 4, respectively) at Elkhorn Slough between 2006 and 2022 (Figure 6). These average rates have taken into account both subsidence (–) and accretion (+) at the Elkhorn Slough watershed. We added the net soil accretion value of every sub-watershed to the post-restoration DEM to generate the future DEMs (i.e., 2050 and 2010) for Elkhorn Slough, which represented the geomorphological changes for the future scenarios (assuming future rates will be similar to those between 2006 and 2022). For example, the surface increasing rate is 1.48 mm/yr in Sub-watershed 1 and its soil accretion will be $1.48/1000 \times (2050–2023) = 0.03996$ m by 2050; similarly for Sub-watersheds 2, 3 and 4, the soil accretions by 2050 will be 0.0486, 0.04239 and 0.06075 m, respectively. This effort addresses distributed surface accretions at Elkhorn Slough for the future scenarios. Accordingly, new meshes were generated based on the 2050 DEM and 2100 DEM, respectively. Similarly, we spun up the model for 1.5 years using a constant tide, followed by 60 days with the corresponding future tidal dataset, to ensure that all the future scenarios (i.e., 2050 with an intermediate SLR scenario, 2050 with a high SLR scenario, 2100 with an intermediate SLR scenario and 2100 with a high SLR scenario) reached equilibrium and minimized the influence of initial conditions prior to conducting the simulations of the future scenarios.

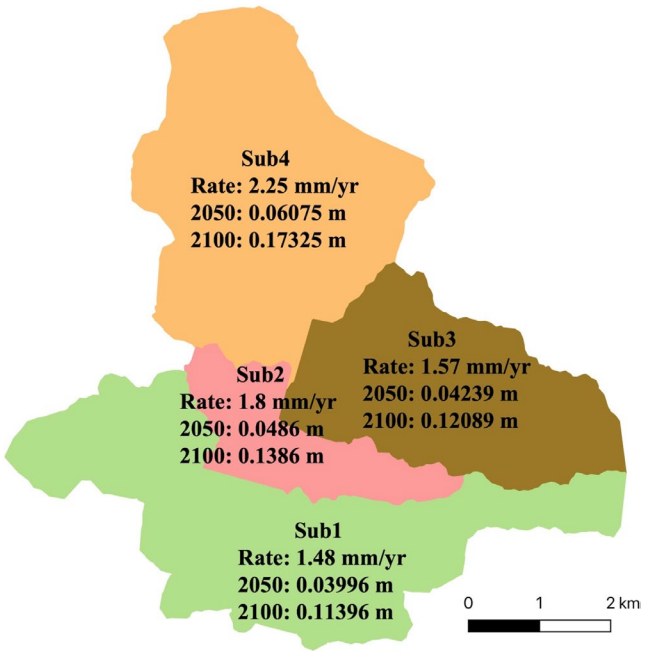

FIGURE 6 | Surface Elevation Tables measurements of average surface increasing rate from 2006 to 2022 (1.48, 1.80, 1.57 and 2.25 mm/yr for Sub-watershed 1, Sub-watershed 2, Sub-watershed 3 and Sub-watershed 4, respectively); and the relevant estimations of surface elevation gains by 2050 and 2100 in the four sub-watersheds at Elkhorn Slough.

3 | Results

3.1 | Model Validation

We validated the model by comparing the surface water depth recorded at two different locations: the watershed outlet (Vierra Mouth) and Hester Marsh. We conducted the model simulations for the first 180 days of 2017 (pre-restoration) and 2023 (post-restoration), considering observation data availability and spanning the wet season in these years.

For the validation at the watershed outlet, to be consistent with the model output, the observed water level elevation at Vierra Mouth (NERRS 2012) was converted to surface water depth for comparison with the simulated values under the pre- and post-restoration scenarios. Figure 7a,b show the comparison of surface water ponded depth between the model simulation and the observation. For visualisation purposes, we only show a record of 30 days. The model performance is similar for all days. Simulation results indicate that ATS effectively captured the temporal dynamics of the daily tidal cycle (i.e., two high tides per day) and the fortnightly cycle (i.e., twice a month neap tides) at the tidal gauge station. The simulated surface water depth closely matched observed values in both pre- and post-restoration scenarios, with the peaks of surface water depths aligning well with observations. The values of root mean square error (RMSE) for surface water depth were 0.21 and 0.22 m for pre- and post-restoration scenarios, respectively. The corresponding Nash–Sutcliffe efficiency (Nash and Sutcliffe 1970) values were 80.0% and 80.4% for the pre- and post-restoration scenarios, respectively, indicating strong agreement between modelled and observed data in terms of both pattern and range. Accurately capturing the daily tidal

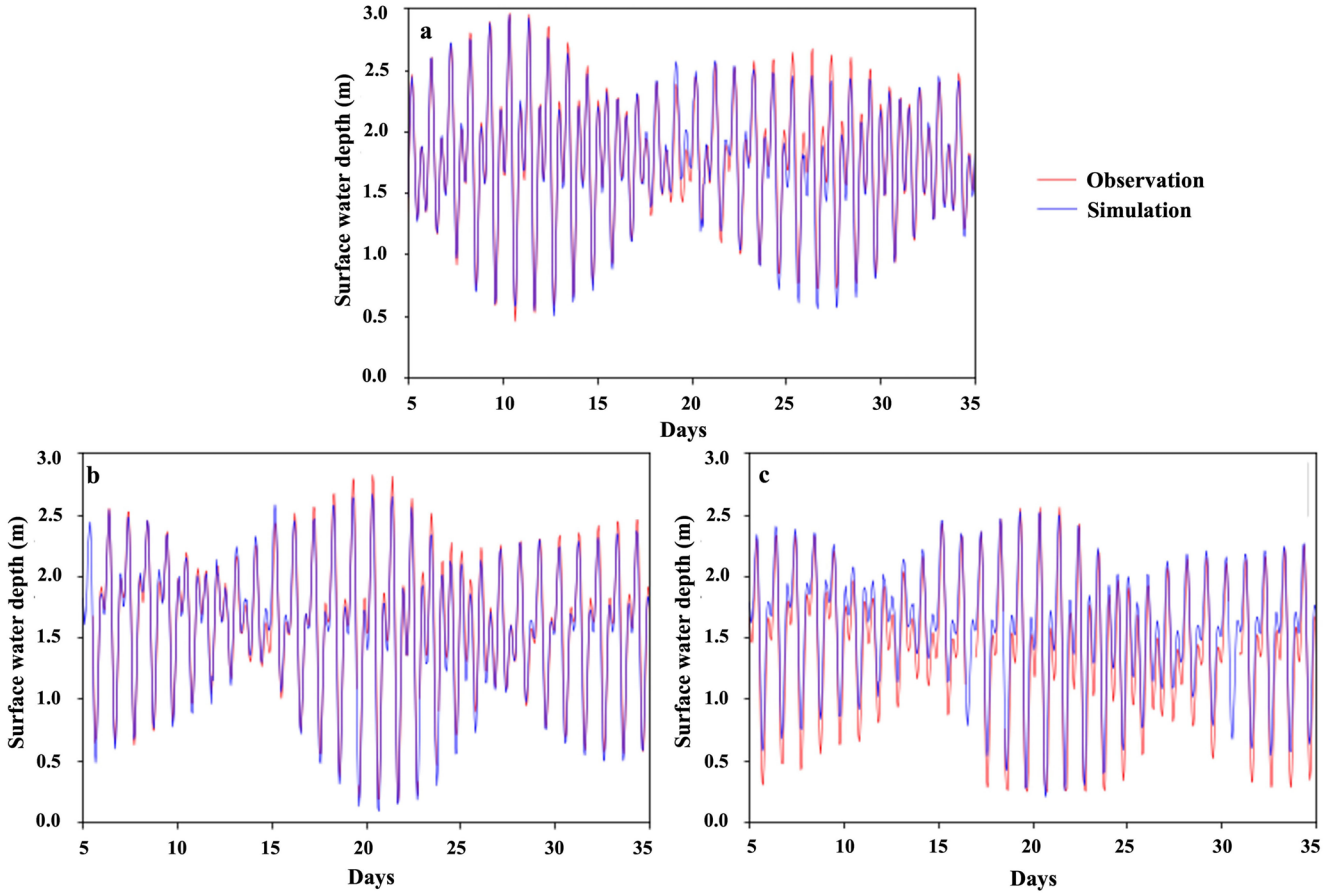

FIGURE 7 | Model validation at the Elkhorn Slough watershed outlet and wetland: (a) the pre-restoration scenario at Vierra Mouth; (b) the post-restoration scenario at Vierra Mouth; Observed surface water depth at Vierra Mouth was calculated as the observed water level (datum: NAVD88) (NERRS 2012) minus the riverbed elevation at Vierra Mouth (−0.6 m, datum: NAVD88) based on bathymetric data; (c) the post-restoration scenario at Hester Marsh.

cycle and fortnightly tidal variations is essential for coastal watershed hydrology, as tides are a primary driver of hydrodynamic processes in these systems.

Since we only had 2 months (i.e., January and February 2023) of available surface water depth observations at Hester Marsh, where a CTD sensor was located near the outlet of Hester Marsh (Figure 1c), we validated the model of hydrodynamics at this marsh by comparing the observed surface water depth and the modelled values in Figure 7c for this duration. Again, we only show a record of 30 days as the model performance for visualisation purposes. Simulation results indicate that ATS can also capture the temporal dynamics of the daily tidal cycle and the fortnightly cycle at Hester Marsh in 2023, especially the high tide values. The simulated low tides were slightly higher than the observation. Some uncertainties may exist in the measurement of surface water depth in the marsh channel, as it was difficult to install the sensor at the bottom of the muddy channel. There is also another potential uncertainty due to the complex topography in this area, such as the narrow and bended channels inside the wetlands which cannot be represented well by the current mesh. The RMSE for daily surface water depth was 0.24 m. The corresponding daily Nash–Sutcliffe efficiency value was 80.3%, indicating a good agreement between modelled and observed data. Overall, the modelling results at Hester Marsh show that the ATS model is able to capture the hydrodynamic processes in the coastal wetland.

3.2 | Coastal Watershed Hydrology

After validating the model simulations, we analyzed the hydrologic characteristics of the watershed by examining the distribution of flood extent and flood time ratio (flood time hours/total hours per year) under different climate conditions in 2017 and 2023. Specifically, flooded area distribution was assessed through the modelled annual average surface water extent and the modelled annual average GWT under the combined impacts of tide and precipitation; flood time ratio was evaluated at the watershed outlet to represent the flood time during a year across the entire watershed.

3.2.1 | Flood Distribution

To examine flood distribution, we determined the spatial distributions of modelled annual average surface water (i.e., flood extent) and the corresponding modelled annual average GWT in the pre–(2017) and post-restoration (2023) scenarios (Figure 8).

The modelled annual average flooded area in the post-restoration scenario (Figure 8c) closely resembled the modelled annual average flood extent in the pre-restoration scenario (Figure 8a) when considering the entire watershed. The restoration project did not show significant impacts on the entire watershed scale. When considering the restored area (i.e., Hester Marsh) a smaller annual average flood extent was indicated in the post-restoration scenario compared to the pre-restoration scenario with spatial variability within the Hester Marsh (Figure 8a,c). The difference in surface water depth between the pre- and post-restoration scenarios was not easily identified in the entire watershed, even though we used a small scale (i.e., 0–0.3 m). But a significant difference was found by focusing on the specific marsh areas in Section 3.3.1.

The spatial distribution of the modelled annual average GWT exhibited a few more differences between the pre- and post-restoration scenarios (Figure 8b,d, respectively), both in the restored area (Phase 1 and Phase 2 Hester Marsh) and in some areas near water bodies (the dashed line polygons in Figure 8b,d). Similar to the surface flood extent comparison, a notable distinction due to the enhanced surface elevation, was shown in the modelled annual average GWT of Phase 1 and Phase 2 Hester Marsh, where the post-restoration condition (Figure 8d) resulted in deeper GWTs below the surface compared to the pre-restoration scenario (Figure 8b). However, compared to the surface flood extent (Figure 8a,c), the modelled annual average GWT was deeper and drier in more polygons in the pre-restoration scenario (Figure 8b) than in the post-restoration scenario (Figure 8d).

3.2.2 | Flood Time Ratio

The modelled flood time ratios in a year for the pre- and post-restoration scenarios are summarised in Table 3. Flood events were classified using five thresholds defined relative to a reference value at the Vierra Mouth (VM_R, set at 2.0 m), which was slightly higher than the modelled average surface water depth and was selected to more effectively capture significant flood events. The five thresholds correspond to exceedances of: (1) at least 0.1 m above VM_R, (2) at least 0.2 m above VM_R, (3) at least 0.3 m above VM_R, (4) at least 0.4 m above VM_R, and (5) at least 0.5 m above VM_R. Under the pre-restoration condition, flood time ratios were 14.4%, 9.3%, 5.5%, 2.7% and 1.3% for surface water depths of 2.1, 2.2, 2.3, 2.4, and 2.5 m, respectively,

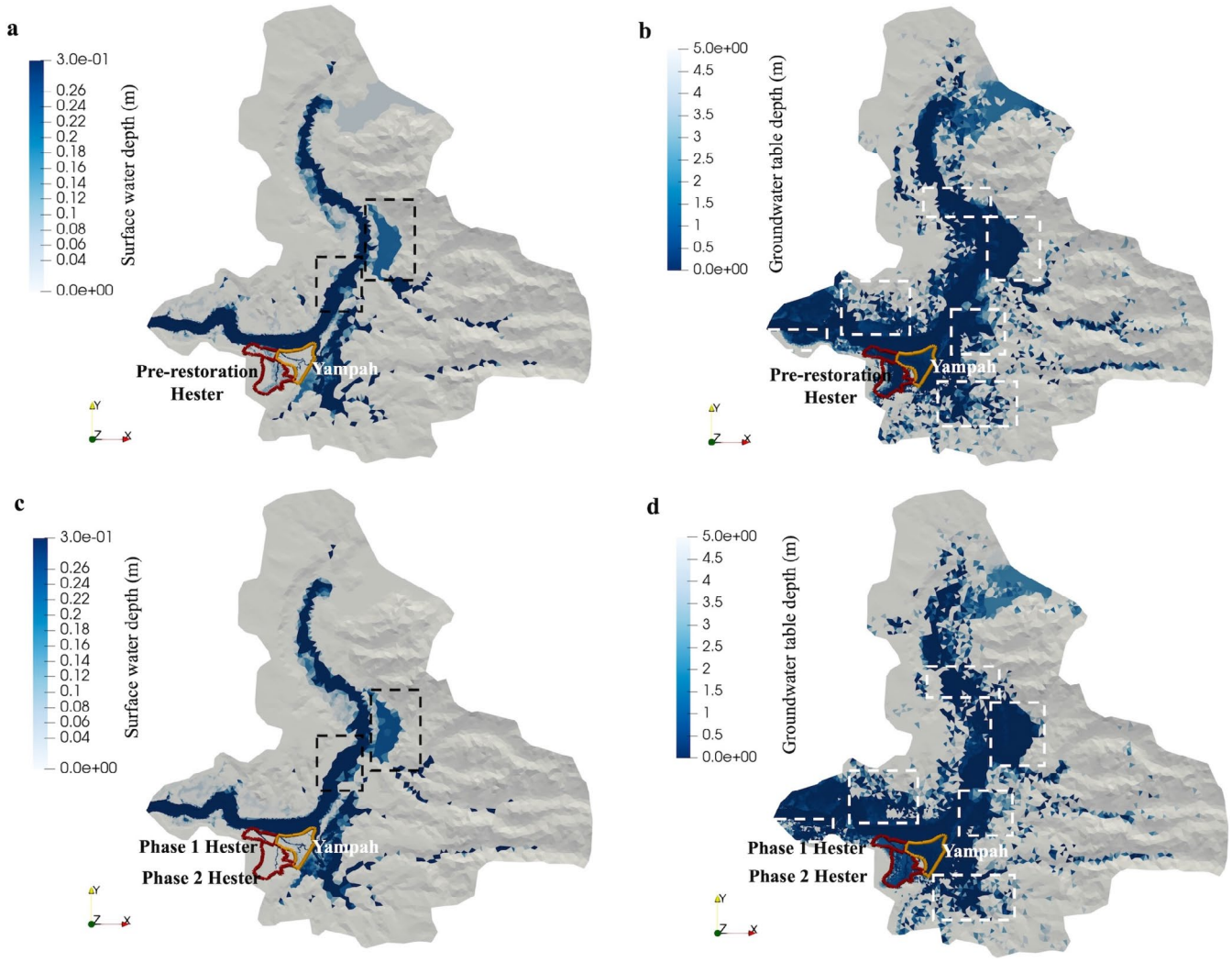

FIGURE 8 | Modelled annual average surface water depth and modelled annual average GWT in ESW: (a) pre-restoration surface water depth; (b) pre-restoration GWT; (c) post-restoration surface water depth; and (d) post-restoration GWT.

TABLE 3 | The modelled flood time ratio at the Vierra Mouth in the pre- (2017) and post-restoration (2023) scenarios.

Flood threshold	0.1 m above VM_R	0.2 m above VM_R	0.3 m above VM_R	0.4 m above VM_R	0.5 m above VM_R
Surface water depth (m)	2.1	2.2	2.3	2.4	2.5
Flood time ratio (%) (pre- restoration)	14.4	9.3	5.5	2.7	1.3
Flood time ratio (%) (post- restoration)	14.3	9.9	6.2	3.5	1.6

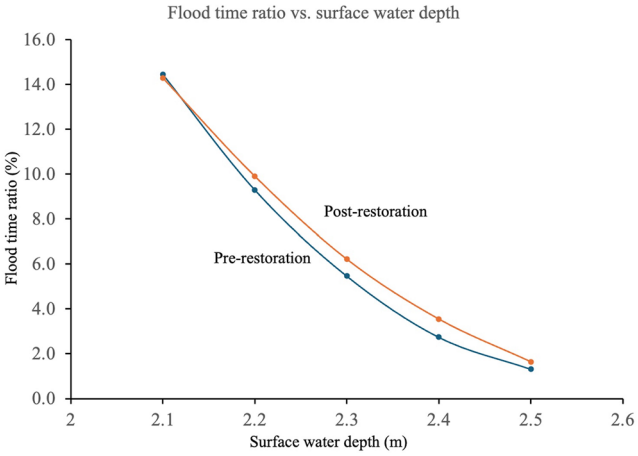

FIGURE 9 | Relationship between flood time ratio and surface water depth (Vierra Mouth) in the pre (2017) and post-restoration (2023) scenarios.

at the Vierra Mouth. In the post-restoration scenario, the corresponding flood time ratios were 14.3%, 9.9%, 6.2%, 3.5% and 1.6%, respectively. It is important to note that the average surface water depth exhibits significant spatial variability near the watershed outlet and selecting an alternative reference location may yield different flood classifications.

The comparison of the relationship between surface water depth and the flood time ratio in the pre- and post-restoration scenarios (Figure 9) indicates that, for the same surface water depth at the Vierra Mouth, the flood time ratio was relatively higher in the post-restoration scenario than in the pre-restoration scenario when surface water depth was deeper than 2.1 m at the Vierra Mouth.

3.3 | Effects of Restoration on Wetland Hydrology

To assess the impact of restoration on wetland hydrology, we analysed flood extent (during the highest tide event in the post-restoration scenario and the same high tide event in the pre-restoration scenario) and daily vertical surface water depth (across the wetlands) at Yampah and Hester, comparing the pre- and post-restoration scenarios.

3.3.1 | Comparison of Flood Extent Before and After Restoration

The highest tide (2.18 m) in the post-restoration scenario occurred on January 5, 2023, at 9:00 AM, while the corresponding similarly high tide in the pre-restoration period was recorded on January 10, 2017, at 08:00 A.M. Figure 10a,b show the simulated flood extent during these high tide events in the pre- and post-restoration scenarios, respectively. To enhance the visualization of the inundated area, the flood extent was presented on a $\log_{10}$ scale for the wetlands case.

The modelled flood extents suggest that the restoration project was able to reduce the flooded area considerably at Hester Marsh. Before wetland restoration, most of the low-elevation areas (north and east sides) in Hester Marsh were inundated during this high tide event (Figure 10a). On the other hand, the modelled inundation extent was smaller, and the surface water depth was also shallower (most of the surface ponded depth was less than 0.1 m except for the Hester channel area) after the wetland restoration (Figure 10b). For Yampah Marsh, the natural wetland site in which elevation has not changed much between 2017 and 2023, the difference in flood extent during this high tide event between the 2 years was not as significant as at Hester Marsh, and nearly all of Yampah Marsh was submerged during the highest tide event.

Although Figure 10 illustrates the impact of wetland restoration on the spatial distribution of surface water at the two wetlands, it represents only a single high-tide event. To provide a broader assessment, we compared daily surface water depth across wetlands between the pre- and post-restoration scenarios.

3.3.2 | Comparison of Surface Water Depth Before and After Restoration

The impact of restoration on surface water depth at Hester Marsh compared to Yampah Marsh is shown in Figure 11. The range of daily surface water depth variation between Hester and Yampah (i.e., daily average surface water depth at Hester—daily average surface water depth at Yampah) in the pre-restoration scenario was −0.02 to 0.12 m, while the range was −0.17 to −0.01 m in the post-restoration scenario. These ranges may be underestimated due to using the daily average values. Overall, the difference in daily average surface water depth between Hester Marsh and Yampah Marsh varied significantly between the pre- and post-restoration scenarios. In the pre-restoration scenario, this difference was predominantly positive, indicating higher surface water depths at Hester Marsh. In contrast, in the post-restoration scenario, the difference became negative, suggesting that surface water depths at Yampah Marsh exceeded those at the restored Hester Marsh. This is because most of the surface elevation at Hester Marsh (except the western hilly area) was lower than Yampah Marsh in the pre-restoration scenario.

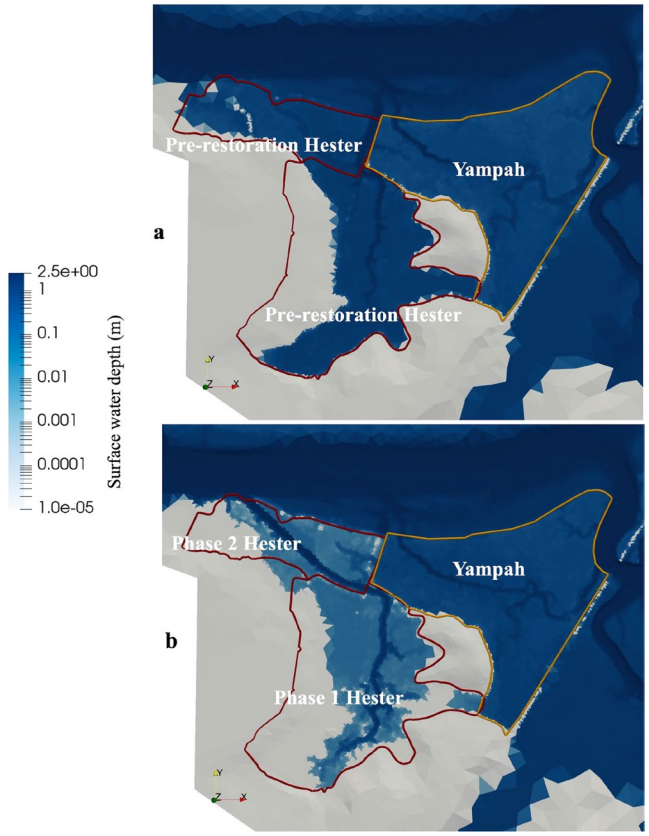

FIGURE 10 | Comparison of the modelled flood extents at Yampah Marsh and Hester Marsh during the high tide of 2.18 m: (a) on January 10, 2017, at 8:00 AM in the pre-restoration scenario and (b) on January 5, 2023, at 9:00 AM in the post-restoration scenario.

Post-restoration, the surface elevation at the east side of Phase 1 Hester Marsh and throughout Phase 2 Hester Marsh has significantly increased due to sediment addition, raising it above the surface elevation of Yampah Marsh. In other words, the Hester Marsh restoration project has a significant impact on maintaining Hester Marsh surface elevation and reducing surface flood inundation.

3.4 | Flood Distribution in Future Scenarios Under SLR

To assess the effectiveness of restoration efforts in enhancing wetland ecosystem functions under future SLR, this study evaluated the resilience of the restored wetland to projected SLR scenarios during both highest and lowest tidal conditions for the years 2050 and 2100. Examining these two contrasting tidal extremes helps us better understand how the natural wetland will look and the capacity of the restored wetland to persist under future SLR.

3.4.1 | Flood Extent During the Highest Tide

We analysed the simulated flood extents during the highest tide corresponding to the same date as in 2023 (January 5 at 9:00 AM) at Yampah Marsh and Hester Marsh for the years 2050 and 2100. This assessment was conducted under both intermediate and high projected SLR scenarios, as illustrated in Figure 12. Temporary submergence of marsh vegetation during high tide conditions is a normal process for many coastal wetlands, in contrast to permanent constant submergence, which would result in the loss of terrestrial marsh vegetation.

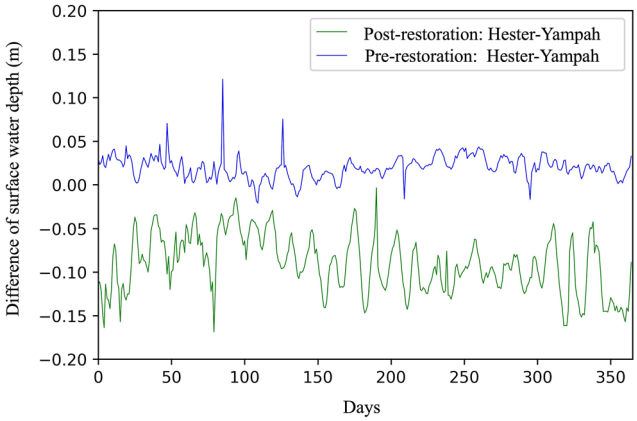

FIGURE 11 | Difference of daily average surface water depth between Hester and Yampah (i.e., daily average surface water depth at Hester—daily average surface water depth at Yampah) in the pre- and post-restoration scenarios.

In 2050, around 99.4% of Yampah Marsh is projected to be submerged during the highest tide (2.46 m) under the high SLR scenario (Figure 12b). Under the intermediate SLR scenario, approximately 99.1% of the marsh will be submerged during the highest tide (2.32 m) (Figure 12a). In contrast, the model results indicate that a higher percentage of Hester Marsh will remain above water under both intermediate and high SLR scenarios in 2050 (Figure 12a,b, respectively). For instance, approximately 94.3% of Phase 2 Hester Marsh will be submerged during the highest tide under the high SLR scenario (Figure 12b). Around 77.1% of Phase 1 Hester Marsh will be inundated under the high SLR scenario (Figure 12b). The flooded proportion of the Hester Marsh will be even smaller under the intermediate SLR scenario in 2050 (Figure 12a).

In 2100, Yampah Marsh is projected to be completely submerged during the highest tide (4.05 m) under the high SLR scenario (Figure 12d). Under the intermediate SLR scenario, Yampah Marsh will also be completely submerged during the highest tide (3.00 m) (Figure 12c). Regarding the restored site, similar to 2050, a higher percentage of Hester Marsh will remain above water under both intermediate and high SLR scenarios in 2100. Around 83.0% of Phase 1 Hester Marsh and 96.5% of Phase 2 Hester Marsh will be submerged under the intermediate SLR scenario in 2100. A greater extent of Hester Marsh will be inundated during the highest tide under the high SLR scenario, with 87.7% of Phase 1 and 98.5% of Phase 2 submerged (Figure 12d). We note that these simulations have included both subsidence (–) and surface accretion (+) at the marsh sites.

3.4.2 | Flood Extent During the Lowest Tide

We also examined the modelled flood extents during the lowest tide (i.e., January 21 at 16:00 PM) for the years 2050 and 2100

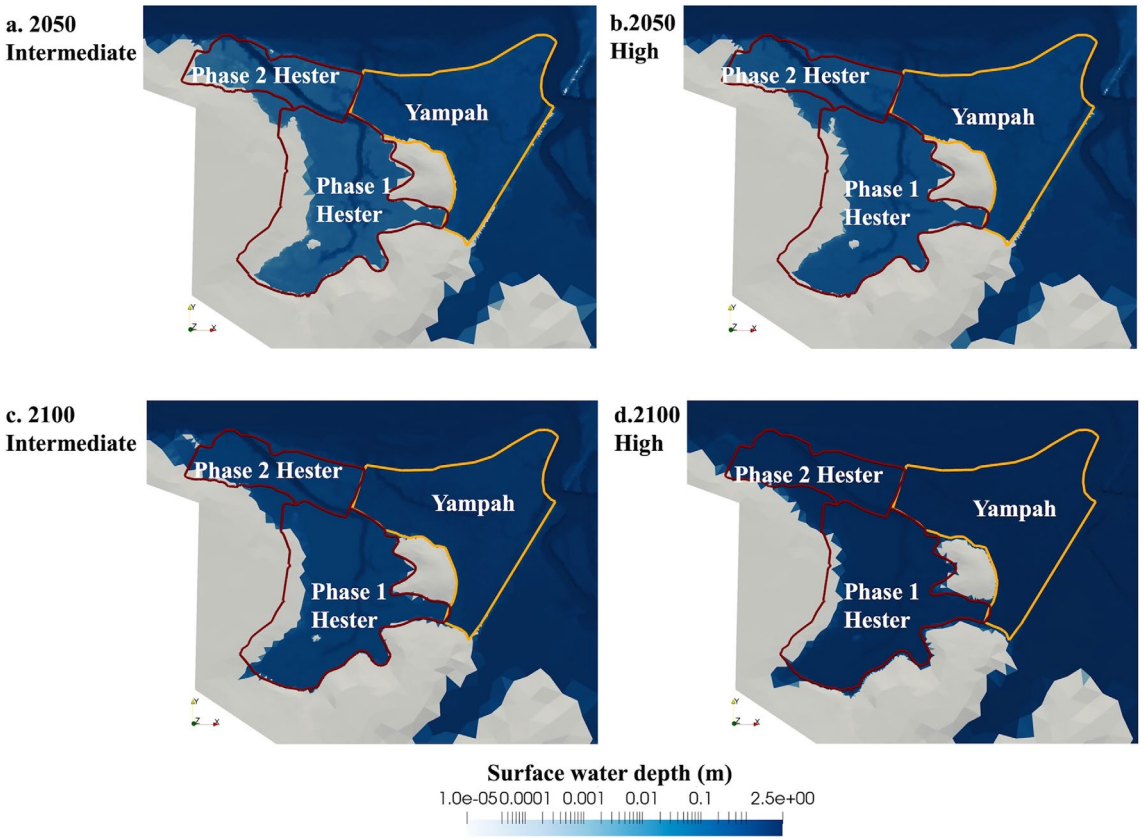

FIGURE 12 | Modelled flood extents at the highest tide under different SLR scenarios: (a) 2050 with an intermediate SLR scenario, highest tidal height of 2.32 m; (b) 2050 with a high SLR scenario, highest tidal height of 2.46 m; (c) 2100 with an intermediate SLR scenario, highest tidal height of 3.00 m; and (d) 2100 with a high SLR scenario, highest tidal height of 4.05 m.

under both intermediate and high SLR scenarios, as shown in Figure 13. At low tide it is expected that marsh vegetation would not be submerged to ensure growth.

In 2050, over 42.5% of Yampah Marsh is projected to be submerged during the lowest tide (−0.25 m) under the high SLR scenario (Figure 13b). Under the intermediate SLR scenario, around 40.3% of the marsh will be submerged during the lowest tide (−0.39 m) (Figure 13a). Regarding the restored site, model results indicate that a lower percentage of Hester Marsh (including 17.4% of Phase 1 and 8.9% of Phase 2) will be inundated under the intermediate SLR scenario in 2050 (Figure 13a), while around 21.9% of Phase 1 and 9.1% of Phase 2 will be submerged under the high SLR scenario (Figure 13b).

In 2100, around 97.8% of Yampah Marsh is projected to be submerged during the lowest tide (1.34 m) under the high SLR scenario (Figure 13d). Under the intermediate SLR scenario, around 51.5% of Yampah Marsh will be submerged during the lowest tide (0.29 m) (Figure 13c). On the restored site, similar to 2050, a lower percentage of Hester Marsh (including 39.1% of Phase 1 and 17.0% of Phase 2) will be inundated by 2100 under the intermediate SLR scenario. About 64.4% of Phase 1 and 41.9% of Phase 2 will be submerged during the lowest tide under the high SLR scenario. These are relatively lower percentages than at Yampah Marsh under the same high SLR scenario. Again, as noted above these calculations have taken into account both subsidence (−) and surface accretion (+) at the marsh sites, assuming net soil accumulation rates do not change in the future.

4 | Discussion

4.1 | Understanding the Impact of Wetland Restoration on Coastal Hydrology

In this study, the primary mechanism by which restoration affected hydrological processes was through soil fill and the enhancement of surface elevation in low-elevation areas of the restored marsh. Consequently, the hydrological functions of the wetland were improved (i.e., less area was inundated permanently allowing marsh vegetation growth).

Surface elevation changes following restoration can significantly influence tidal exchange and hydrodynamics. Specifically, alterations in elevation affect water flow dynamics within tidal marshes, potentially restricting water movement between the Elkhorn Slough main channel and the restored wetland topographic highs. In particular, these changes modify the natural range of surface water depth (Figure 11). The current restoration efforts at Hester Marsh help mitigate prolonged water stagnation, thereby improving wetland function, specifically allowing marsh vegetation to colonize, lowering greenhouse gas emissions.

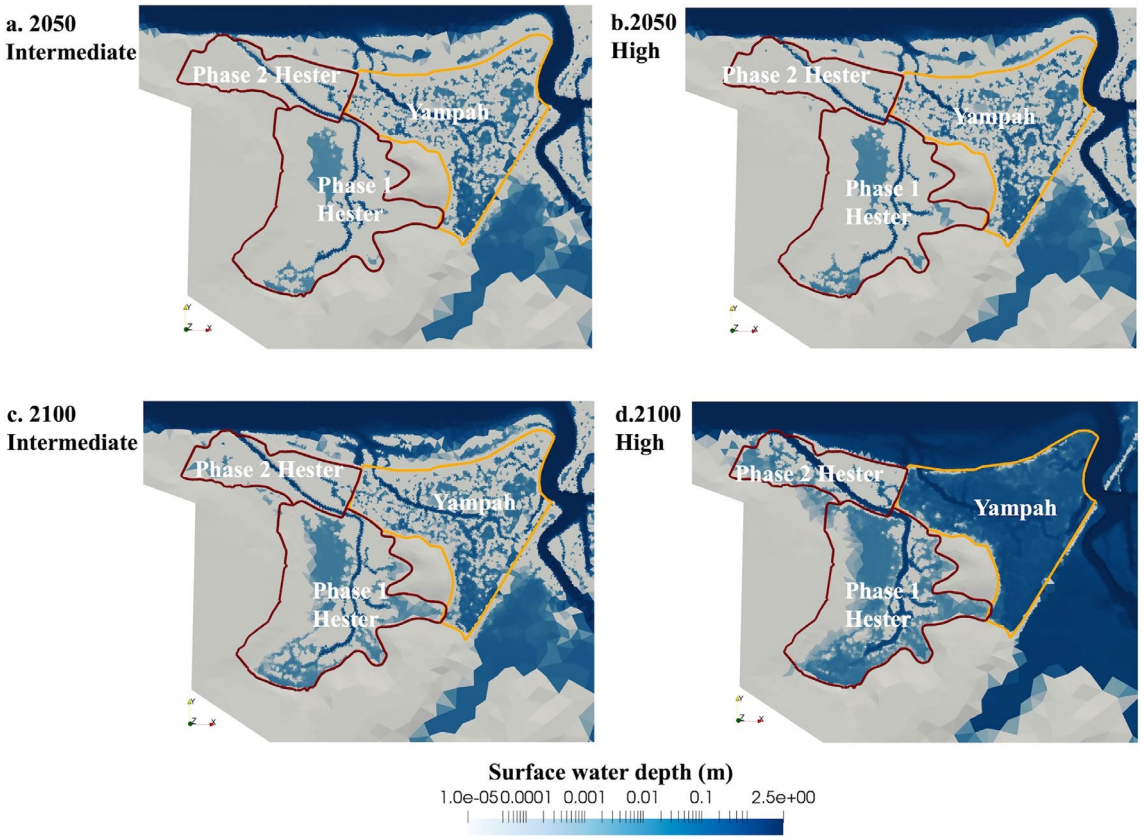

FIGURE 13 | Modelled flood extents at the lowest tide under different SLR scenarios: (a) 2050 with an intermediate SLR scenario, lowest tidal height of −0.39 m; (b) 2050 with a high SLR scenario, lowest tidal height of −0.25 m; (c) 2100 with an intermediate SLR scenario, lowest tidal height of 0.29 m; and (d) 2100 with a high SLR scenario, lowest tidal height of 1.34 m.

The water storage capacity of the restored wetland could be enhanced as well after the surface elevation increased, as additional soil was introduced. This improvement may increase the wetland's ability to retain water, potentially reducing excessive ponding and increasing oxygen penetration to the subsurface. Rather than transitioning into a mudflat in the future, the wetland can better support a diverse range of plant and animal species providing biodiversity function. Further research is needed to prove this by assessing the impact of restoration on subsurface soil movements and soil saturation, which remains a knowledge gap in this study.

Most importantly, model simulations show that the wetland restoration in this study can increase resilience to SLR maintaining the majority of the restored area above sea level. We discussed this in more detail in the next section.

At the watershed scale, the restoration area was too small to induce significant hydrological changes; however some other regions within the watershed showed deeper annual average GWTs (dash line polygons in Figure 8b) in the pre-restoration scenario than the post-restoration scenario (dash line polygons in Figure 8d). The effect of SLR between 2017 and 2023 can extend inland, altering surface inundation dynamics and GWT. Change in precipitation between those 2 years can also reshape GWT and surface water, thereby influencing estuarine circulation. In this study, a potential explanation for the change in those areas (dash line polygons in Figure 8) seems more closely related to SLR between 2017 and 2023. The average tide of 2023 was 3.6% higher than the average tide of 2017, although the pre-restoration year (2017) experienced more precipitation (8.5%) than the post-restoration year (2023). This indicates that SLR may play a more important role than precipitation in causing flood risk at Elkhorn Slough. This finding is consistent with a higher flood time ratio in the post-restoration scenario than the pre-restoration scenario (Figure 9). In addition, previous research indicated that Elkhorn Slough is strongly affected by tidal inputs during certain seasons (Montalvo et al. 2024), which further supports this finding. In contrast, another study based on data from seven marsh sites (including Elkhorn Slough) across the Atlantic, Gulf, and Pacific coasts of the United States found that upland terrestrial hydrology is also one of the primary drivers of salt marsh hydrology (Guimond et al. 2025). Particularly for inland watersheds such as the San Carlos catchment in Costa Rica, headwater dynamics largely control downstream flow during the dry season (Birkel et al. 2020). Therefore, more detailed future research is needed to assess these specific observations and explanations at our site.

4.2 | The Effectiveness of Wetland Restoration Under SLR

Assessing the effects of future SLR provides critical insights into the potential survival of the natural and restored sites (i.e., Yampah Marsh and Hester Marsh). The simulations with the highest tide may indicate a worst-case scenario for the

inundated area at both sites under future SLR. Meanwhile, the simulations with the lowest tides under future SLR may offer a more important perspective because it is likely the areas that will be submerged during the lowest tides of the year will be submerged all the time.

At Yampah Marsh, according to the modelled flood extents at the highest tide under different SLR scenarios (Figure 12), if the marsh surface elevation fails to keep pace with SLR and the high SLR scenario is applied, > 99.0% of the area would be submerged during the highest tide condition (i.e., 2.46 m) in 2050. Even under the intermediate SLR scenario (i.e., a highest tide of 2.32 m), only less than 1.0% of Yampah Marsh will remain above surface water in 2050. This finding is consistent with the field observations indicating that most of Yampah Marsh is inundated when the tidal level (NAVD88) exceeds 2.2 m (Fountain et al. 2020).

The modelled flood extents at the lowest tide under different future SLR scenarios (Figure 13) suggest that, if the natural wetland (i.e., Yampah Marsh) cannot keep pace with SLR, over 40.0% is projected to be inundated all the time under both intermediate and high SLR scenarios in 2050. In particular, if the high SLR scenario is applied, 97.8% of Yampah Marsh will likely be submerged all the time in 2100 and the marsh will become a mudflat. Our modelling results refine a previous empirical study that suggested more than 90.0% of Yampah Marsh would be lost to submergence by 2100 (Wasson et al. 2012). This finding highlights the need for enhancing surface elevation at Yampah Marsh to preserve its vegetation and associated ecosystem services.

At the restored site, around 22.9% of Phase 1 Hester Marsh is expected to retain its capacity to support marsh vegetation during the highest tide under the high SLR scenario in 2050, while only about 5.7% of Phase 2 Hester Marsh is projected to remain above water during the highest tide under the same scenario (Figure 12), likely due to its proximity to the Elkhorn Slough main channel. Thus, the worst-case scenario is that around 18.3% of Hester including both Phase 1 and Phase 2 is expected to remain above water at the highest tide under the high SLR scenario in 2050.

At the same time, approximately 15.2% and 18.5% of the restored area, including Phase 1 and Phase 2, are projected to be submerged at the lowest tide under the intermediate SLR scenario and the high SLR scenario, respectively, in 2050 (Figure 13). In other words, more than 80% of Hester Marsh can remain above water under 0.14 m and 0.28 m of SLR (based on the 2023 baseline) in the two 2050 scenarios. Our finding provides specific quantitative estimates and is consistent with the Hester Marsh restoration report, which indicates that the restored site can accommodate up to 0.5 m of SLR (Fountain et al. 2022). Here, we assumed that no significant tidal change occurred between 2022 and 2023. However, more area (i.e., 58.5%) in Hester Marsh including Phase 1 and Phase 2 is projected to be submerged all the time during the lowest tide under the high SLR scenario in 2100 due to 1.87 m of SLR (based on the 2023 baseline). Overall, Hester Marsh appears to be more capable than Yampah Marsh of maintaining wetland ecosystem functions (e.g., flood risk reduction) under future SLR scenarios, attesting to the success of the restoration project for attaining this goal.

4.3 | Discussion of Uncertainty

4.3.1 | Complex Topography

One of the main sources of uncertainty in this study is the complex topography of the ESW, particularly the narrow and highly meandering channels at Yampah Marsh and Hester Marsh, which are not fully captured by the current mesh resolution.

Significant effort was dedicated to addressing the challenges posed by the complex topography. First, defining an appropriate watershed boundary was crucial for coastal hydrologic modelling (Fringer et al. 2019; Tanim et al. 2024), especially for Elkhorn Slough, due to the complex topography within the watershed, which includes water bodies, natural and restored areas, and upland regions. In particular, the intricate tidal channels of the slough and adjacent water bodies near the watershed outlet could lead to unrealistic ocean water flow into the computational domain, which had to be assessed based on field observations.

Second, it is also essential to note that having a high-resolution DEM which includes detailed bathymetric information plays an important role in ensuring that the model captures the topographic characteristics in coastal areas, as discussed in previous coastal studies (Amante et al. 2023; Loftis et al. 2016; Medeiros et al. 2015). In particular, the shapes and depths of the narrow channels within the tidal marshes at Elkhorn Slough may have large impacts on the water movement and exchange within the marsh. The bathymetric data facilitated the correction of NHDPlus flowlines, improving their alignment with real conditions and enhancing the representation of land surface elevation. Notably, a modification was made to the flowlines at the restored Hester Marsh, where a newly constructed channel was created to connect Hester Marsh to the Elkhorn Slough main channel. The original NHDPlus flowlines did not adequately capture the conditions within this newly established channel.

Finally, a fine-resolution mesh was selected to represent the narrow channels and capture the topographic characteristics of the tidal wetlands at Elkhorn Slough. However, some uncertainties may still arise due to the mesh resolution limitations imposed by computational constraints. The mesh resolution fundamentally governs both the accuracy of the results and the computational efficiency of the model; nevertheless, it cannot fully capture the complexity of bathymetry in many complex coastal regions (Fringer et al. 2019). For instance, our simulation of flood extent at the wetland sites may contain uncertainties due to the mesh resolution limitations. Although the surface mesh resolution in most areas of the tidal marshes (Yampah and Hester) was refined to ~5 to 10 m, it remained insufficient to fully represent variations in the channel bathymetry and hence surface water depth. In this study, further refinement of the mesh was impractical due to computational constraints. However, based on the validation results (Figure 7), we expect these uncertainties to have a limited impact on the overall modelling results, particularly in terms of hydrological patterns and comparison between the

two marshes. Therefore, the overall conclusions drawn in this study remain robust and reliable.

4.3.2 | Other Uncertainties

The current configuration setting of model functions such as evapotranspiration, infiltration, recharge, surface flow and subsurface flow has been included in ATS at a 3D scale, making the model run slowly and requiring extensive computation resources. The model also effectively incorporated tidal dynamics, allowing tidal oscillations to propagate along the Elkhorn Slough River and into the inland wetlands. In this study, we did not consider other potential processes such as the dynamic dependence of sedimentary processes on SLR, due to limitations in computational resources and data availability. For example, biological accretionary processes may probably also increase wetland elevation (Morris et al. 2002; Saintilan et al. 2022; Sun et al. 2024), but they may not be able to keep pace with the most recent SLR. That is one of the reasons why soils were manually added to the restored wetland to increase its surface elevation. Some uncertainties may arise if dynamic processes of biological accretionary or non-linear changes in sediment accretion are not considered. For example, variations in plant productivity and the root-to-shoot ratio can influence the vertical accretion rate in tidal wetlands (Morris et al. 2016). However, we assume these are less significant than the main components represented in the model.

As sea level increases in the future scenarios, the rate of elevation gain will likely increase due to more frequent inundation than the historical situation or channel scouring may reduce sediment accretion. Incorporating more dynamic processes within the model may be necessary to better capture sediment accretion.

Additionally, we acknowledge that the diffusion-wave approximation does not fully capture the complexity of estuarine hydrodynamics, particularly in deeper or more tidally energetic sections of the estuary. Our modelling framework, however, was designed to emphasise surface–subsurface interactions across the upland and low-gradient tidal zones, where diffusive flow is representative of system behaviour. The diffusion-wave approach also provides computational efficiency and numerical stability, both of which are essential for long-term simulations and coupling with groundwater processes.

Furthermore, water level was used for model calibration in this study. However, such calibration does not uniquely constrain internal hydrodynamic processes. Incorporating tracer data into the calibration could provide complementary information, particularly regarding water storage, flow paths and transit times (Birkel and Soulsby 2015). Therefore, a more robust calibration approach is recommended for future work.

5 | Conclusions and Future Work

This study presents ATS as a useful model to investigate the impacts of coastal wetland restoration on hydrological processes at the Elkhorn Slough watershed with a focus on comparison between a nearby natural wetland and a restored wetland. The model was successfully set up and configured by comparing the simulation results with available field observations. The high-resolution nature of ATS makes it possible to capture the characteristics of the hydrological processes at the entire watershed and represent the impact of restoration within specific marsh sites. The model validation shows that ATS performed well, capturing the daily tidal cycle and the fortnightly cycle seen in available observations.

The modelled annual average flood distribution and flood time ratio in ESW indicates that annual average water increased in the post-restoration year compared to the pre-restoration year, possibly reflecting the impact of SLR in the past decade. The restoration impact on the watershed scale hydrology was not significant, since the restoration area only covered a small portion of the ESW. However, future SLR is likely to increase flood risk throughout the watershed.

At the wetland site scale, the flood extent in the post-restoration scenario showed a smaller flooded area at the restored site following restoration. Our results suggest that the restoration project which included increasing the site's elevation effectively protected the restored wetland (i.e., Hester Marsh) reducing tidal water inundation, restoring marsh habitat and its ecosystem services. This suggests that maintaining marsh surface elevation above expected future SLR reduces flood risks and enhances coastal resilience.

There are some key findings for the effectiveness of wetland restoration under future SLR: (1) it is necessary to consider enhancing surface elevation as part of restoration to ensure that the vegetated wetland does not become submerged and transition into a mudflat; (2) assessment of resilience using models in the face of SLR requires high-resolution DEM, bathymetry and sediment accretion data.

Our future work will focus on minimizing uncertainties caused by complex topography to enhance simulation accuracy at the marsh sites through a more data-driven approach. Additionally, we will explore methods to address dynamic geomorphological changes in future scenarios.

Acknowledgements

This research was supported by funds from the UC National Laboratory Fees Research Program of the University of California, Grant Number L22CR4529. Coastal Wetland Restoration is a Nature-Based Decarbonization Multi-Benefit Climate Mitigation Solution. The authors would like to thank Paytan Biogeochemistry Lab at University of California Santa Cruz for providing necessary measurements at the marshes. We also thank Michael Wilshire for his efforts on the measurement of soil texture for the post-restoration soil. We thank Dr. Xi Zhang, Dr. Brant Robertson and Josh Sonstroem for their help on computing related issues at UC Santa Cruz and for providing computing resources. We acknowledge the use of the lux supercomputer at UC Santa Cruz, funded by NSF MRI grant AST 1828315. This research also used the Lawrencium computational cluster resource provided by the IT Division at the Lawrence Berkeley National Laboratory (supported by the Director, Office of Science, Office of Basic Energy Sciences, of the U.S. Department of Energy under Contract No. DE-AC02-05CH11231).

Funding

This work was supported by the UC National Laboratory Fees Research Program of the University of California, Grant Number L22CR4529.

Data Availability Statement

The datasets used in this study can be found on ESS-DIVE: https://doi.org/10.15485/2588510 (Xu et al. 2025). The Advanced Terrestrial Simulator (Coon et al. 2019) is open source under the three-clause BSD licence and is publicly available at https://github.com/amanzi/ats. Simulations were conducted using version 1.4.2.

References

Acreman, M., J. Fisher, C. Stratford, D. Mould, and J. Mountford. 2007. "Hydrological Science and Wetland Restoration: Some Case Studies From Europe." *Hydrology and Earth System Sciences* 11, no. 1: 158–169.

Amante, C. J., M. Love, K. Carignan, M. G. Sutherland, M. MacFerrin, and E. Lim. 2023. "Continuously Updated Digital Elevation Models (CUDEMs) to Support Coastal Inundation Modeling." *Remote Sensing* 15, no. 6: 1702.

Ardón, M., J. L. Morse, B. P. Colman, and E. S. Bernhardt. 2013. "Drought-Induced Saltwater Incursion Leads to Increased Wetland Nitrogen Export." *Global Change Biology* 19, no. 10: 2976–2985.

Arias-Ortiz, A., P. Y. Oikawa, J. Carlin, et al. 2021. "Tidal and Nontidal Marsh Restoration: A Trade-Off Between Carbon Sequestration, Methane Emissions, and Soil Accretion." *Journal of Geophysical Research – Biogeosciences* 126, no. 12: e2021JG006573.

Arnold, J. G., R. Srinivasan, R. S. Muttiah, and J. R. Williams. 1998. "Large Area Hydrologic Modeling and Assessment Part I: Model Development 1." *JAWRA Journal of the American Water Resources Association* 34, no. 1: 73–89.

Barbier, E. B. 2013. "Valuing Ecosystem Services for Coastal Wetland Protection and Restoration: Progress and Challenges." *Resources* 2, no. 3: 213–230.

Birkel, C., A. Correa-Barahona, M. Martinez-Martinez, et al. 2020. "Headwaters Drive Streamflow and Lowland Tracer Export in a Large-Scale Humid Tropical Catchment." *Hydrological Processes* 34, no. 18: 3824–3841.

Birkel, C., and C. Soulsby. 2015. "Advancing Tracer-Aided Rainfall–Runoff Modelling: A Review of Progress, Problems and Unrealised Potential." *Hydrological Processes* 29, no. 25: 5227–5240.

Cadier, C., E. Bayraktarov, R. Piccolo, and M. F. Adame. 2020. "Indicators of Coastal Wetlands Restoration Success: A Systematic Review." *Frontiers in Marine Science* 7: 600220.

Caffrey, J., M. Brown, W. B. Tyler, and M. Silberstein. 2002. *Changes in a California Estuary: A Profile of Elkhorn Slough*. Elkhorn Slough Foundation.

Cavalcante, G., F. Vieira, E. Campos, N. Brandini, and P. R. Medeiros. 2020. "Temporal Streamflow Reduction and Impact on the Salt Dynamics of the São Francisco River Estuary and Adjacent Coastal Zone (NE/Brazil)." *Regional Studies in Marine Science* 38: 101363.

Coon, E. T., J. D. Moulton, E. Kikinzon, et al. 2020. "Coupling Surface Flow and Subsurface Flow in Complex Soil Structures Using Mimetic Finite Differences." *Advances in Water Resources* 144: 103701.

Coon, E. T., J. D. Moulton, and S. L. Painter. 2016. "Managing Complexity in Simulations of Land Surface and Near-Surface Processes." *Environmental Modelling & Software* 78: 134–149.

Coon, E. T., and P. Shuai. 2022. "Watershed Workflow: A Toolset for Parameterizing Data-Intensive, Integrated Hydrologic Models." *Environmental Modelling & Software* 157: 105502.

Coon, E. T., D. Svyatsky, A. Jan, et al. 2019. *Advanced Terrestrial Simulator (ATS). [Computer Software]*. US DOE Office of Science (SC), Biological and Environmental Research (BER). https://doi.org/10.11578/dc.20190911.1.

Costanza, R., O. Pérez-Maqueo, M. L. Martinez, P. Sutton, S. J. Anderson, and K. Mulder. 2008. "The Value of Coastal Wetlands for Hurricane Protection." *Ambio* 37: 241–248.

County of Monterey. 2024. "Flooding and Winter Storms." https://www.readymontereycounty.org/prepare/flooding-and-winter-storms.

Dai, Z., C. C. Trettin, C. Li, D. M. Amatya, G. Sun, and H. Li. 2010. "Sensitivity of Stream Flow and Water Table Depth to Potential Climatic Variability in a Coastal Forested Watershed 1." *JAWRA Journal of the American Water Resources Association* 46, no. 5: 1036–1048.

Dhi, D. 2005. "MIKE SHE Technical Reference." Version 2005. DHI Water and Environment.

Eagle, M. J., K. D. Kroeger, A. C. Spivak, et al. 2022. "Soil Carbon Consequences of Historic Hydrologic Impairment and Recent Restoration in Coastal Wetlands." *Science of the Total Environment* 848: 157682.

Fountain, M., C. Endris, A. Woolfolk, and K. Wasson. 2020. "Salt Marsh Conservation, Restoration and Enhancement Opportunities in and Around Elkhorn Slough in the Face of Sea Level Rise." Elkhorn Slough Technical Report Series 2020, 2.

Fountain, M., R. Jeppesen, C. Endris, et al. 2022. "Hester Marsh Restoration." Annual Report. Elkhorn Slough National Estuarine Research.

Fringer, O. B., C. N. Dawson, R. He, D. K. Ralston, and Y. J. Zhang. 2019. "The Future of Coastal and Estuarine Modeling: Findings From a Workshop." *Ocean Modelling* 143: 101458.

Ghazal, K. A., O. T. Leta, A. I. El-Kadi, and H. Dulai. 2020. "Impact of Coastal Wetland Restoration Plan on the Water Balance Components of Heeia Watershed, Hawaii." *Hydrology* 7, no. 4: 86.

Grande, E., B. Arora, A. Visser, et al. 2022. "Tidal Frequencies and Quasiperiodic Subsurface Water Level Variations Dominate Redox Dynamics in a Salt Marsh System." *Hydrological Processes* 36, no. 5: e14587.

Grande, E., E. C. Seybold, C. Tatariw, et al. 2023. "Seasonal and Tidal Variations in Hydrologic Inputs Drive Salt Marsh Porewater Nitrate Dynamics." *Hydrological Processes* 37, no. 8: e14951.

Guimond, J. A., E. Grande, H. A. Michael, et al. 2025. "The Hidden Influence of Terrestrial Groundwater on Salt Marsh Function and Resilience." *Nature Water* 3: 1–166.

Harris, B. D., A. Ostojic, L. P. Tedesco, et al. 2025. "Wetland Elevation Change Following Beneficial Use of Dredged Material Nourishment." *Frontiers in Ecology and Evolution* 13: 1518759.

Homer, C. G., J. A. Fry, and C. A. Barnes. 2012. *The National Land Cover Database (Nos. 2327–6932)*. US Geological Survey.

Huscroft, J., T. Gleeson, J. Hartmann, and J. Börker. 2018a. "Compiling and Mapping Global Permeability of the Unconsolidated and Consolidated Earth: GLobal HYdrogeology MaPS 2.0 (GLHYMPS 2.0)." [Dataset]. https://doi.org/10.5683/SP2/TTJNIU.

Huscroft, J., T. Gleeson, J. Hartmann, and J. Börker. 2018b. "Compiling and Mapping Global Permeability of the Unconsolidated and Consolidated Earth: GLobal HYdrogeology MaPS 2.0 (GLHYMPS 2.0)." *Geophysical Research Letters* 45, no. 4: 1897–1904.

Kennish, M. J. 2002. "Environmental Threats and Environmental Future of Estuaries." *Environmental Conservation* 29, no. 1: 78–107.

Lal, A. W. 1998. "Weighted Implicit Finite-Volume Model for Overland Flow." *Journal of Hydraulic Engineering* 124, no. 9: 941–950.

Li, L., D. Barry, and C. Pattiaratchi. 1997. "Numerical Modelling of Tide-Induced Beach Water Table Fluctuations." *Coastal Engineering* 30, no. 1–2: 105–123.

Li, X., R. Bellerby, C. Craft, and S. E. Widney. 2018. "Coastal Wetland Loss, Consequences, and Challenges for Restoration." *Anthropocene Coasts* 1, no. 1: 1–15.

Loftis, J. D., H. V. Wang, R. J. DeYoung, and W. B. Ball. 2016. "Using Lidar Elevation Data to Develop a Topobathymetric Digital Elevation Model for Sub-Grid Inundation Modeling at Langley Research Center." *Journal of Coastal Research* 76: 134–148.

McDonald, M. G., and A. W. Harbaugh. 1988. *A Modular Three-Dimensional Finite-Difference Ground-Water Flow Model*. US Geological Survey.

Medeiros, S., S. Hagen, J. Weishampel, and J. Angelo. 2015. "Adjusting Lidar-Derived Digital Terrain Models in Coastal Marshes Based on Estimated Aboveground Biomass Density." *Remote Sensing* 7, no. 4: 3507–3525.

Montalvo, M. S., E. Grande, A. E. Braswell, et al. 2024. "A Fresh Take: Seasonal Changes in Terrestrial Freshwater Inputs Impact Salt Marsh Hydrology and Vegetation Dynamics." *Estuaries and Coasts* 47, no. 8: 2389–2405.

Morris, J. T., D. C. Barber, J. C. Callaway, et al. 2016. "Contributions of Organic and Inorganic Matter to Sediment Volume and Accretion in Tidal Wetlands at Steady State." *Earth's Future* 4, no. 4: 110–121.

Morris, J. T., D. R. Cahoon, J. C. Callaway, C. Craft, S. C. Neubauer, and N. B. Weston. 2021. "Marsh Equilibrium Theory: Implications for Responses to Rising Sea Level." In *Salt Marshes: Function, Dynamics, and Stresses*, edited by D. M. FitzGerald and Z. J. Hughes, 157–177. Cambridge University Press.

Morris, J. T., J. Z. Drexler, L. J. Vaughn, and A. H. Robinson. 2022. "An Assessment of Future Tidal Marsh Resilience in the San Francisco Estuary Through Modeling and Quantifiable Metrics of Sustainability." *Frontiers in Environmental Science* 10: 1039143.

Morris, J. T., P. Sundareshwar, C. T. Nietch, B. Kjerfve, and D. R. Cahoon. 2002. "Responses of Coastal Wetlands to Rising Sea Level." *Ecology* 83, no. 10: 2869–2877.

Nash, J. E., and J. V. Sutcliffe. 1970. "River Flow Forecasting Through Conceptual Models Part I—A Discussion of Principles." *Journal of Hydrology* 10, no. 3: 282–290.

NERRS. 2012. "NOAA National Estuarine Research Reserve System (NERRS). System-Wide Monitoring Program." Data Accessed From the NOAA NERRS Centralized Data Management Office Website. http://www.nerrsdata.org.

Newton, A., T. J. Carruthers, and J. Icely. 2012. "The Coastal Syndromes and Hotspots on the Coast." *Estuarine, Coastal and Shelf Science* 96: 39–47.

Nicholls, R. J., F. M. Hoozemans, and M. Marchand. 1999. "Increasing Flood Risk and Wetland Losses due to Global Sea-Level Rise: Regional and Global Analyses." *Global Environmental Change* 9: S69–S87.

Niu, L., H. Cai, L. Jia, et al. 2021. "Metal Pollution in the Pearl River Estuary and Implications for Estuary Management: The Influence of Hydrological Connectivity Associated With Estuarine Mixing." *Ecotoxicology and Environmental Safety* 225: 112747.

Office for Coastal Management. 2025. "2009—2011 CA Coastal Conservancy Coastal Lidar Project." https://www.fisheries.noaa.gov/inport/item/48166.

Priestley, C. H. B., and R. J. Taylor. 1972. "On the Assessment of Surface Heat Flux and Evaporation Using Large-Scale Parameters." *Monthly Weather Review* 100, no. 2: 81–92.

Richards, L. A. 1931. "Capillary Conduction of Liquids Through Porous Mediums." *Physics* 1, no. 5: 318–333.

Saintilan, N., K. E. Kovalenko, G. Guntenspergen, et al. 2022. "Constraints on the Adjustment of Tidal Marshes to Accelerating Sea Level Rise." *Science* 377, no. 6605: 523–527.

Shangguan, W., T. Hengl, J. Mendes de Jesus, H. Yuan, and Y. Dai. 2017. "Mapping the Global Depth to Bedrock for Land Surface Modeling." *Journal of Advances in Modeling Earth Systems* 9, no. 1: 65–88.

Simley, J. D., and W. J. Carswell Jr. 2009. *The National Map-Hydrography (Nos 2327–6932)*. US Geological Survey.

Soil Survey Staff. 2021. *National Resources Conservation Service. United States Department of Agriculture*. Web Soil Survey. https://websoilsurvey.nrcs.usda.gov/.

Sun, G., H. Riekerk, and N. B. Comerford. 1998. "Modeling the Hydrologic Impacts of Forest Harvesting on Florida Flatwoods 1." *JAWRA Journal of the American Water Resources Association* 34, no. 4: 843–854.

Sun, Y., K. Rogers, K. K. Lal, and N. Saintilan. 2024. "Living Root Contributions Dominate Vertical Accretion, but Not Carbon Burial, in Two SE Australian Tidal Wetlands." *Estuarine, Coastal and Shelf Science* 302: 108776.

Sweet, W. V., B. D. Hamlington, R. E. Kopp, et al. 2022. "Global and Regional Sea Level Rise Scenarios for the United States: Updated Mean Projections and Extreme Weather Level Probabilities Along US Coastlines."

Tanim, A. H., F. W. McKinnie, and E. Goharian. 2024. "Coastal Compound Flood Simulation Through Coupled Multidimensional Modeling Framework." *Journal of Hydrology* 630: 130691.

Turner, R. E., and R. Lewis. 1996. "Hydrologic Restoration of Coastal Wetlands." *Wetlands Ecology and Management* 4: 65–72.

Vreugdenhil, C. B. 1994. *Numerical Methods for Shallow-Water Flow*. Vol. 13. Springer Science & Business Media.

Wasson, K., B. Suarez, A. Akhavan, et al. 2015. "Lessons Learned From an Ecosystem-Based Management Approach to Restoration of a California Estuary." *Marine Policy* 58: 60–70.

Wasson, K., E. Watson, E. Van Dyke, G. Hayes, and I. Aiello. 2012. "A Novel Approach Combining Rapid Paleoecological Assessments With Geospatial Modeling and Visualization to Help Coastal Managers Design Salt Marsh Conservation Strategies in the Face of Environmental Change." Elkhorn Slough Technical Report Series.

Watson, E. B., K. Wasson, G. B. Pasternack, et al. 2011. "Applications From Paleoecology to Environmental Management and Restoration in a Dynamic Coastal Environment." *Restoration Ecology* 19, no. 6: 765–775.

Xia, Y., K. Mitchell, M. Ek, et al. 2012. "Continental-Scale Water and Energy Flux Analysis and Validation for the North American Land Data Assimilation System Project Phase 2 (NLDAS-2): 1. Intercomparison and Application of Model Products." *Journal of Geophysical Research: Atmospheres* 117, no. D3: 2011JD016048. https://doi.org/10.1029/2011JD016048.

Xu, Y., Y. Zhang, J. D. Moulton, et al. 2025. "Data-Model Files Associated With the Manuscript 'Modeling the Effects of Wetland Restoration on Coastal Hydrology: A Case Study of Elkhorn Slough Watershed, California'." Coastal Wetland Restoration a Nature Based Decarbonization Multi-Benefit Climate Mitigation Solution, [Dataset]. ESS-DIVE Repository. https://doi.org/10.15485/2588510.

Yu, M., E. Rivera-Ocasio, T. Heartsill-Scalley, D. Davila-Casanova, N. Rios-López, and Q. Gao. 2019. "Landscape-Level Consequences of Rising Sea-Level on Coastal Wetlands: Saltwater Intrusion Drives Displacement and Mortality in the Twenty-First Century." *Wetlands* 39, no. 6: 1343–1355.

Zhang, B., T. Zheng, X. Zheng, et al. 2023. "Dynamics of Upstream Saltwater Intrusion Driven by Tidal River in Coastal Aquifers." *Science of the Total Environment* 877: 162857.

Zhang, Y., W. Li, G. Sun, et al. 2018. "Understanding Coastal Wetland Hydrology With a New Regional-Scale, Process-Based Hydrological Model." *Hydrological Processes* 32, no. 20: 3158–3173.

Zhang, Y., W. Li, G. Sun, and J. S. King. 2019. "Coastal Wetland Resilience to Climate Variability: A Hydrologic Perspective." *Journal of Hydrology* 568: 275–284.

Zhang, Y., D. Svyatsky, J. C. Rowland, et al. 2022. "Impact of Coastal Marsh Eco-Geomorphologic Change on Saltwater Intrusion Under Future Sea Level Rise." *Water Resources Research* 58, no. 5: e2021WR030333.